bound to the ER may leak into the cytosolic fraction during the preparation of homogenates.

Identification of Carboxylesterase Isozyme Involved in the Hydrolysis of Butyryl-PL. The microsomes from rat and dog tissues were subjected to SDS-PAGE and transferred electrophoretically to nitrocellulose for immunostaining. Anti-D1 polyclonal antibody, a specific antibody for dog liver carboxylesterase (D1), was used to detect the presence of the enzyme. In the results of immunostaining (Fig. 7), 60-kDa proteins were expressed in the lung and kidney but not in the small intestine in dogs. The cytosol showed an immunoblotting pattern similar to that of microsomes in dog tissues (data not shown), which supports the idea that carboxylesterase leaks from the microsomes during the preparation of homogenates. The 60-kDa protein was also expressed in the rat liver and lung but not in the rat small intestine. This protein might be a D1 cross-reactive carboxylesterase. Moreover, a protein of higher molecular weight was observed in the rat kidney.

The inhibition profiles of hydrolase activities for each enantiomer of butyryl PL by anti-D1 polyclonal antibody are shown in Fig. 8. The control rabbit IgG did not have any influence on the hydrolase activity for butyryl-PL of the dog liver or lung microsomes, but specific anti-D1 polyclonal antibody inhibited 70% of the hydrolysis of both enantiomers of butyryl-PL in the liver and showed nearly complete inhibition in the lung. These findings indicate that D1 or cross-reactive carboxylesterases catalyze the hydrolysis of butyryl-PL in dog liver and lung. However, no inhibition by anti-D1-antibody was observed in the hydrolysis of butyryl-PL in rat liver microsomes.

Discussion

Carboxylesterases play an important role in the metabolism of endogenous compounds and exogenous substances such as drugs (including prodrugs), pesticides, and herbicides. Carboxylesterases are widely distributed in the microsomes of the several tissues such as liver, kidney, brain, and lung, where they are loosely bound to the luminal surface of the ER. The highest concentration of carboxylesterases is found in the liver microsomes (Morgan et al., 1994). Furthermore, it has been reported that secretory form such as serum carboxylesterase is highly expressed in rodent (Yan et al., 1995b). Therefore, the in vivo hydrolysis of drug containing ester moiety depends on hydrolase activity in the tissues as well as the blood.

Taking into account the drug disposition after administration, hydrophilic drugs are mainly distributed to the systemic blood circulation, whereas hydrophobic drugs distribute in several tissues. The hydrophobicity and basicity of butyryl-PL strongly suggest that butyryl-PL is distributed to several tissues, including the lung. Therefore, the blood concentrations of PL and butyryl-PL may be regulated by the hydrolytic activity in the respective tissues in each species. In fact, the markedly low blood levels of butyryl-PL observed after the intravenous administration of racemic butyryl-PL in dogs could not explain the hydrolysis in the blood but the rapid hydrolysis of butyryl-PL in several tissues (Table 2).

It has been reported that PL is taken up into the lung by simple diffusion in the dog and that the lung has a capacity for 50 to 60% first-pass uptake of PL (Pang et al., 1982). About 25% of administered PL accumulates in the isolated rat lung during a 5-min perfusion period through simple diffusion and a saturable pathway (Dollery and Junod, 1976). Therefore, butyryl-PL might also be taken up into the lung due to its higher hydrophobicity and similar basicity compared with PL. However, the intravenous administration of butyryl-PL resulted in marked differences in disposition in rats and dogs (Fig. 2). This divergence was mainly due to differences in pulmonary hydrolase activity in rats and dogs. In particular, dogs showed pulmonary first-pass hydrolysis in which about 50% of the administered butyryl-PL was hydrolyzed (Fig. 4). Furthermore, the hydrolysis of butyryl-PL in the liver and kidney at nearly same rate as tissue blood flow led to the rapid and complete conversion of butyryl-PL to PL in the dogs. However, rats showed the only 30% of conversion of butyryl-PL to PL up to 2 h after intravenous administration, and the plasma concentrations of both butyryl-PL and PL were much lower than the plasma PL concentration when PL was administered to rats. These observations suggest that, in the rat, butyryl-PL is distributed to various tissues, including the lung, where esterase activity for butyryl-PL is low (Table 2). After distribution to various tissues in the rat, butyryl-PL can remain in tissues with little hydrolase activity until it diffuse back into the blood and/or is detoxified to other metabolites. Furthermore, if butyryl-PL flows into the liver, which expresses esterase and P450, it may be sequentially metabolized to PL-metabolites after hydrolysis. The intrinsic clearance of PL for its P450 metabolism in the rat liver has been reported to be 810 l/h/kg (Ishida et al., 1992) and 1,690 to 2,260 l/h/kg (Gariépy et al., 1992) in in vitro experiments using rat liver microsomes and isolated perfused liver, respectively. Because these values are much larger than the intrinsic clearance by the hydrolysis of butyryl-PL in the rat liver (Table 3), PL is readily metabolized after the hydrolysis of butyryl-PL. The low PL concentration after the intravenous administration of butyryl-PL to the rat could be explained by retention in nonmetabolizing tissues followed by sequential metabolism in the liver, which is the only major hydrolyzing tissue for butyryl-PL.

It has been demonstrated that the esterase responsible for pulmonary hydrolysis is D1 based on Western immunoblotting and the inhibition by anti-D1 antibody (Figs. 7 and 8). Carboxylesterase D1 is grouped in the CES-1 family according to the classification system proposed by Satoh and Hosokawa (1998). D1 is also expressed in the dog liver and

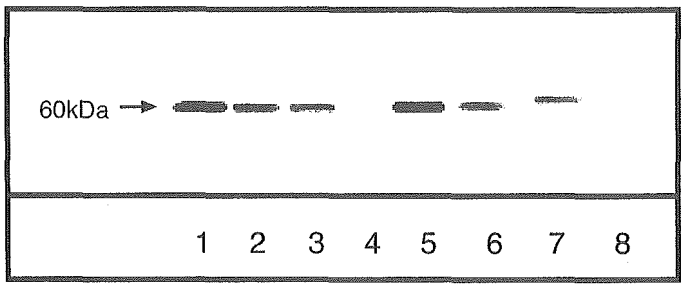

Fig. 7. Immunoblots of microsomes from various tissues of the rat and dog probed with anti-D1 IgG. Microsomes from rat and dog tissues were subjected to SDS-PAGE and transferred electrophoretically to nitrocellulose for immunostaining. Lanes 1 to 8 contained 5 μg of protein. Lane 1, dog liver; lane 2, dog lung; lane 3, dog kidney; lane 4, dog small intestine; lane 5, rat liver; lane 6, rat lung; lane 7, rat kidney; and lane 8, rat small intestine.

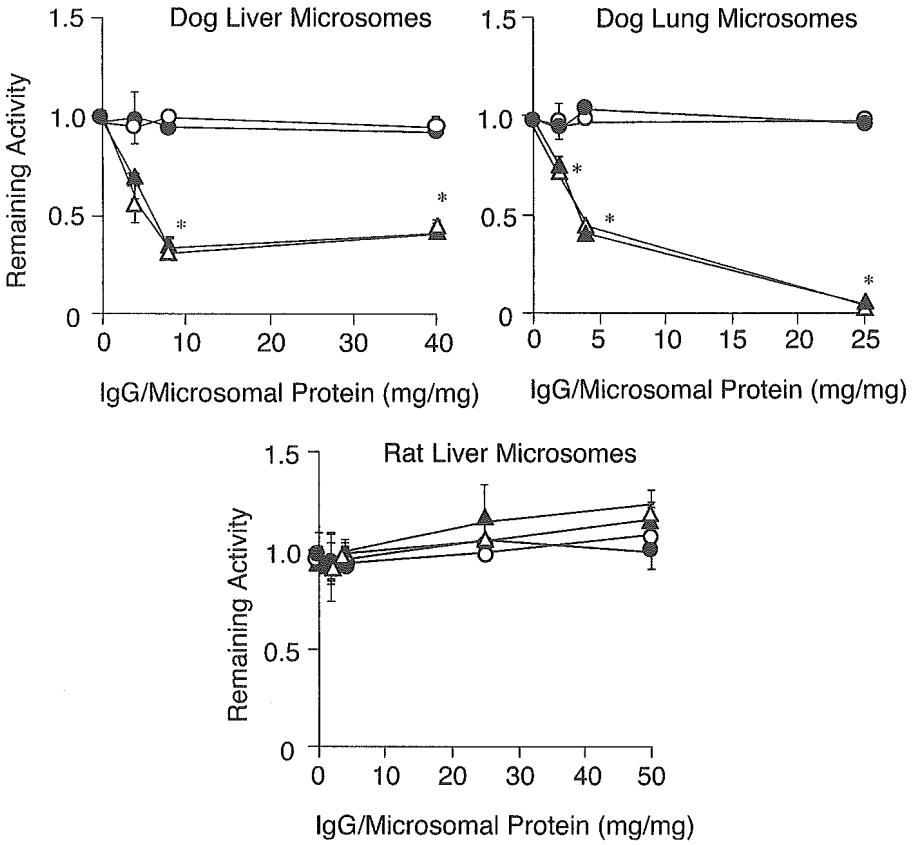

Fig. 8. Effects of polyclonal anti-D1 antibodies on the hydrolase activities for each butyryl PL enantiomer in dog liver and lung microsomes and in rat liver microsomes. Remaining activity values [open symbols, (*R*)-isomer; closed symbols, (*S*)-isomer] were plotted against the ratio of protein contents of IgG and microsomes. Circles and triangles indicate the presence of rabbit IgG (control) and anti-D1 IgG, respectively. Values are the mean ± S.D. (n = 3). *, $p < 0.05$ compared with rabbit IgG (control).

kidney and catalyzes the hydrolysis of butyryl-PL to PL (Table 3). Western immunoblotting showed the presence of a cross-reacting enzyme against anti-D1 antibody in rat tissues. RH-1, RL-1, and hydrolase S, which are in the CES-1 family, are found in the rat lung. Particularly RH-1 is abundantly expressed in the lung (Gaustad et al., 1991; Yan et al., 1995a; Barr et al., 1998). On the other hand, the high levels of RL-1 in the kidney make it possible to evaluate its activity from the hydrolase activity in kidney microsomes. It has been reported that the molecular weight of RL-1 is 61 kDa, in contrast to 58 kDa for RH-1 (Hosokawa et al., 1987). In fact, the cross-reacting protein with anti-D1 antibody in the rat kidney showed a band at a higher molecular weight in Western immunoblotting (Fig. 7). Interestingly, butyryl-PL could not be hydrolyzed in the rat lung and kidney, indicating that RH-1 and RL-1 do not recognize butyryl-PL as a substrate despite their 78 and 66% homology with D1, respectively (Hosokawa et al., 2001). Actually, it has been reported that the hydrolysis of butyryl-PL in rat liver microsomes is not inhibited by anti-RH-1 antibody (Yoshigae et al., 1999). Hosokawa et al. (1990) have reported that RL-2 presents as a CES-1 isozyme in the rat liver and that RL-2 is characterized by its specific hydrolysis of 1-acyl glycerols (monoglycerides). A possible explanation for the hepatic hydrolysis of butyryl-PL might be the participation of RL-2.

In addition, rat esterase recognizes butyryl-PL as a specific substrate not only in the liver but also in the small intestine (Yoshigae et al., 1998a). It is clear that CES-2 enzymes can catalyze the hydrolysis of butyryl-PL, because the CES-2 isozyme is highly express in the small intestine. The homology of CES-2 enzymes with CES-1 enzymes is less than 50%, and the isoelectric point of the CES-2 family (4.0–5.0) is lower than that of the CES-1 family (5.0–6.0). In general, both CES-1 and CES-2 enzymes are expressed in the liver of all mammalian species. The CES-2 enzyme also catalyzes the hydrolysis of butyryl-PL in rat liver microsomes. However, the major enzyme for hydrolysis of butyryl-PL is not CES-2 enzyme, because the enantioselectivity of the hydrolysis of butyryl-PL in the rat small intestine homogenate was opposite that observed in the liver (Yoshigae et al., 1998b). Further experiments are necessary to identify the CES isozyme responsible for the hydrolysis of butyryl-PL in the rat liver.

Similarly, the CES-2 isozyme is expressed in the dog liver and kidney. As shown in Fig. 6, the lower band in PAGE electrophoresis corresponds to the CES-2 enzyme. The finding that the hydrolase activity for butyryl-PL in the dog liver showed 70% inhibition by anti-D1 antibody despite complete inhibition by BNPP could be explained by the presence of D2, a dog CES-2 family carboxylesterase, contributory to the hydrolysis of butyryl-PL (Figs. 5 and 8). Moreover, D2 was also observed to contribute to the hydrolysis of butyryl-PL when the hydrolytic activities for butyryl-PL and PNPA were compared in dog lung and kidney microsomes. The ratios of the hydrolysis of PNPA to that of butyryl-PL were 47 and 10 for lung microsomes and kidney microsomes, respectively (Table 2). Because the kidney, which contains both D1 and D2, was found to have a smaller value than the lung, which contains only D1, D2 might extensively catalyze the hydrolysis of butyryl-PL. With regard to the overlap in substrate specificity, it is interesting that butyryl-PL is not hydrolyzed by RH-1 and RL-1, which are grouped in the CES-1 family, despite the fact that CES-2 enzymes, which have less than 50% homology with the CES-1 family, also recognize butyryl-PL as a substrate.

The findings of the present study have demonstrated that pulmonary esterase activity is influenced by the disposition of drugs containing an ester-bond and that the species differences in pulmonary esterase activity are based on substrate specificities. A possible carboxylesterase that is present in the human lung is HU-1, a member of the CES-1 family, which has 78% homology with D1 (Munger et al., 1991; Satoh and Hosokawa, 1998). It has been demonstrated that butyryl-PL is a good substrate for HU-1, which is found extensively in the human liver (Satoh and Hosokawa, 1998). These findings suggest the presence of first-pass metabolism of butyryl-PL in the human lung.

In addition to hydrolase activity in the liver and plasma, pulmonary metabolism is important in the elimination of drugs, but has rarely been studied due to problems inherent in the experimental methodologies currently available. Although in vivo methods have been applied to directly assess pulmonary first-pass metabolism in experimental animals, pulmonary metabolism can also be determined indirectly by conducting in vitro metabolic experiments using lung homogenates. Moreover, commercially available human lung preparations are useful for evaluating pulmonary metabolism and for predicting the disposition of ester-containing drugs in human. Further kinetic studies concerning pulmonary metabolism are required to establish a suitable model for describing pulmonary metabolism in vivo.

References

Ahmed S, Imai T, Yoshigae Y, and Otagiri M (1997) Stereospecific activity and nature of metabolizing esterases for propranolol prodrug in hairless mouse skin liver and plasma. *Life Sci* **61:**1879–1887.

Barr F, Clark H, and Hawgod S (1998) Identification of a putative surfactant convertase in rat lung as a secreted serine carboxylesterase. *Am J Physiol* **274:** L404–L410.

Dean RA, Zhang J, Brzezinski MR, and Bosron WF (1995) Tissue distribution of cocaine methyl esterase and ethyltransferase activities: correlation with carboxylesterase protein. *J Pharmacol Exp Ther* **275:**965–971.

Dollery CT and Junod AF (1976) Concentration of (±)-propranolol in isolated, perfused lungs of rat. *Br J Pharmacol* **57:**67–71.

Forkert P-G, Lee RP, and Reis K (2001) Involvement of CYP2E1 and carboxylesterase enzymes in vinyl carbamate metabolism in human lung microsomes. *Drug Metab Dispos* **29:**258–263.

Gariépy L, Fenyves D, and Villeneuve J-P (1992) Propranolol disposition in the rat: variation in hepatic extraction with unbound drug fraction. *J Pharm Sci* **81:**255–258.

Gaustad R, Sletten K, Lovhaug D, and Fonnum F (1991) Purification and characterization of carboxylesterases from rat lung. *Biochem J* **274:**693–697.

George CF, Orme M L'E, Burabapong P, Macerlean D, Breckenridge AM, and Dollery CT (1976) Contribution of the liver to overall elimination of propranolol. *J. Pharmacokinet Biopharm* **4:**17–27.

Heymann E (1982) Hydrolysis of carboxylic esters and amides, in *Metabolic Basis of Detoxification* (Jakoby WB, Bend JR, and Caldwell J eds) pp 229–245, Academic Press, New York.

Hosokawa M, Maki T, and Satoh T (1987) Multiplicity and regulation of hepatic microsomal carboxylesterases in rats. *Mol Pharmacol* **31:**579–584.

Hosokawa M, Maki T, and Satoh T (1990) Characterization of molecular species of liver microsomal carboxylesterases of several animal species and humans. *Arch Biochem Biophys* **277:**219–227.

Hosokawa M, Suzuki K, Takahashi D, Mori M, Satoh T, and Chiba K (2001) Purification, molecular cloning and functional expression of dog liver microsomal acyl-CoA hydrolase: a member of the carboxylesterase multigene family. *Arch Biochem Biophys* **389:**245–253.

Ishida R, Suzuki K, Masubuchi Y, Narimatsu S, Fujita S, and Suzuki T (1992) Enzymatic basis for the non-linearity of hepatic elimination of propranolol in the isolated perfused rat liver. *Biochem Pharmacol* **44:**2281–2288.

Iwamoto K and Watanabe J (1985) Dose-dependent presystemic elimination of propranolol due to hepatic first-pass metabolism in rats. *J Pharm Pharmacol* **37:**826–828.

Lowry OH, Rosebrough NJ, Farr AL, and Randall RJ (1951) Protein measurement with the folin phenol reagent. *J Biol Chem* **193:**264–275.

McCracken NW, Blain PG, and Williams FM (1993) Nature and role of xenobiotic metabolizing esterases in rat liver, lung, skin and blood. *Biochem Pharmacol* **45:**31–36.

Mentlein R, Heiland S, and Heymann E (1980) Simultaneous purification and comparative characterization of six serine hydrolases from rat liver microsomes. *Arch Biochem Biophys* **200:**547–559.

Morgan EW, Yan B, Greenway D, Petersen DR, and Parkinson A (1994) Purification and characterization of two rat liver microsomal carboxylesterase (hydrolase A and B). *Arch Biochem Biophys* **315:**495–512.

Munger JS, Shi GP, Mark EA, Chin DT, Gerard C, and Chapman HA (1991) A serine esterase released by human alveolar macrophages is closely related to liver microsomal carboxylesterase. *J Biol Chem* **266:**18832–18838.

Nambu K, Miyazaki H, Nakanishi Y, Oh-e Y, and Matsunaga Y (1987) Enzymatic hydrolysis of haloperidol decanoate and its inhibition by proteins. *Biochem Pharmacol* **36:**1715–1722.

Pang JA, Blackburn JP, Butl and RJ, Corrin B, Williams TR, and Geddes DM (1982) Propranolol uptake by dog lung: effect of pulmonary artery occlusion and shock lung. *J Appl Physiol Respiratory Environ Exer Physiol* **52:**393–401.

Prueksaritanont T, Gorham LM, Hochman JH, Tran LO, and Vyas KP (1996) Comparative studies of drug-metabolizing enzymes in dog, monkey, and human small intestines and Caco-2 cells. *Drug Metab Dispos* **24:**634-642.

Prueksaritanont T, Gorham LM, and Yeh KC (1997) Analysis of metabolite kinetics by deconvolution and in vivo-in vitro correlations of metabolite formation rates: studies of fibrinogen receptor antagonist ester prodrugs. *J Pharm Sci* **86:**1345–1351.

Satoh T (1987) Role of carboxylesterases in xenobiotic metabolism, in *Reviews in Biochemical Toxicology* (Benda JR, Hodgston BE, and Philpot RM eds) pp 155–181, Elsevier, New York.

Satoh T and Hosokawa M (1998) The mammalian carboxylesterases: from molecule to functions. *Annu Rev Pharmacol Toxicol* **38:**257–288.

Shameem M, Imai T, and Otagiri M (1993) An in-vitro and in-vivo correlative approach to the evaluation of ester prodrugs to improve oral delivery of propranolol. *J Pharm Pharmacol* **45:**246–252.

Tsujita T, Miyata T, and Okuda H (1988) Purification of rat kidney carboxylesterase and its comparison with other tissue esterases. *J Biochem* **103:**327–331.

Tsujita T and Okuda H (1993) Palmitoyl-coenzyme A hydrolyzing activity in rat kidney and its relationship to carboxylesterase. *J Lipid Res* **34:**1773–1781.

Van Lith HA, Haller M, Van Zutphen LF, and Beynen AC (1992) The use of three Ferguson-plot-based calculation methods to determine the molecular mass of proteins as illustrated by molecular mass assessment of rat-plasma carboxylesterase ES-1, ES-2 and ES-14. *Anal Biochem* **201:**288–300.

Vermeulen M, Belpaire FM, Moerman E, Smet F, and Bogaert MG (1992) The influence of aging on the stereoselective pharmacokinetics of propranolol in the rat. *Chirality* **4:**473–479.

Yan B, Yang D, Brady M, and Parkinson A (1995a) Rat testicular carboxylesterase: cloning, cellular localization and relationship to liver hydrolase A. *Arch Biochem Biophys* **316:**899–908.

Yan B, Yang D, Bullock P, and Parkinson A (1995b) Rat serum carboxylesterase; cloning, expression, regulation and evidence of secretion from liver. *J Biol Chem* **270:**19128–19134.

Yoshigae Y, Imai T, Aso T, and Otagiri M (1998a) Species differences in the disposition of propranolol prodrugs derived from hydrolase activity in intestinal mucosa. *Life Sci* **62:**1231–1241.

Yoshigae Y, Imai T, Horita A, Matsukane H, and Otagiri M (1998b) Species differences in stereoselective hydrolase activity in intestinal mucosa. *Pharm Res (NY)* **15:**626–631.

Yoshigae Y, Imai T, Horita A, and Otagiri M (1997) Species differences for stereoselective hydrolysis of propranolol prodrugs in plasma and liver. *Chirality* **9:**661–666.

Yoshigae Y, Imai T, Taketani M, and Otagiri M (1999) Characterization of esterases involved in the stereoselective hydrolysis of ester-type prodrugs of propranolol in rat liver and plasma. *Chirality* **11:**10–13.

Address correspondence to: Dr. Teruko Imai, Faculty of Pharmaceutical Sciences, Kumamoto University, 5-1 Oe-honmachi, Kumamoto 862-0973, Japan. E-mail: iteruko@gpo.kumamoto-u.ac.jp

Available online at www.sciencedirect.com
SCIENCE DIRECT®
European Journal of Pharmacology 477 (2003) 137–141
ejp
www.elsevier.com/locate/ejphar

Effects of α_1-acid glycoprotein on isometric tension of mouse aorta

Yoshiko Tokutomi[a], Shigehiro Okamoto[b], Kazuaki Matsumoto[b], Masaki Otagiri[b], Katsuhide Nishi[a], Naofumi Tokutomi[a,*]

[a] *Department of Pharmacology, Kumamoto University School of Medicine, 2-2-1 Honjo, Kumamoto 860-0811, Japan*
[b] *Faculty of Pharmaceutical Sciences, Kumamoto University, Kumamoto 862-0973, Japan*

Received 23 May 2003; received in revised form 16 July 2003; accepted 22 July 2003

Abstract

We examined the effects of human α_1-acid glycoprotein on isometric tension of mouse aortic rings. α_1-Acid glycoprotein (7.5–75 μM) produced a transient, concentration-dependent relaxation of the phenylephrine-precontracted preparation. Although N^G-nitro-L-arginine methyl ester or removal of endothelium rarely affected the α_1-acid glycoprotein-induced relaxation, extracellular heparin inhibited the α_1-acid glycoprotein-induced relaxation. In 10 mM Ca^{2+}-containing external solutions, the α_1-acid glycoprotein-induced relaxation was significantly potentiated. In the 60 mM KCl-precontracted preparation, α_1-acid glycoprotein produced weaker relaxation than in the phenylephrine-precontracted preparation. These results suggest that the vasorelaxant effect of α_1-acid glycoprotein is mainly achieved by block of Ca^{2+} entry in the vascular smooth muscle cells. The interaction between α_1-acid glycoprotein molecules and plasmalemmal Ca^{2+} entry channels may be modified by extracellular Ca^{2+} and heparin.

Keywords: α_1-Acid glycoprotein; Aorta, mouse; Isometric tension; Ca^{2+} entry; Smooth muscle cell, vascular

1. Introduction

α_1-Acid glycoprotein is one of the major acute phase reactants in plasma during inflammation (Kremer et al., 1988). The plasma level of human α_1-acid glycoprotein (10–25 μM under physiological conditions) increases several-fold in inflammation and cancer, after surgery and during pregnancy. Although many biological activities of α_1-acid glycoprotein have been described (Bennett and Schmid, 1980; Fournier et al., 2000), most of the underlying mechanisms remain uncertain. Both α_1-acid glycoprotein and its mRNA were constitutively expressed in primary cultures of human microvascular endothelial cells from dermal tissue (Sorensson et al., 1999). Maeda et al. (1980) demonstrated that human α_1-acid glycoprotein promoted the passage of erythrocytes through a membrane-filter of 3 μm in pore size and exhibited a protecting effect against hemolysis during filtration. In terms of protection against tissue damage, such as inflammation, cancer, surgery and pregnancy, the facility of circulation of blood in the tissue is an important issue.

The present study was designed to determine whether α_1-acid glycoprotein has possibility to influence the circulation of blood at the site of acute phase reaction and to know the underlying mechanism accordingly. Thus, we tested the effects of α_1-acid glycoprotein on isometric tension of mouse aortic rings.

2. Materials and methods

Descending thoracic aortae were excised from BALB/c mice (6–8 weeks old) immediately after decapitation under ether anaesthesia. The aorta was trimmed free of loosely adhering connective tissue and fat and cut into 2-mm-long rings. The ring was mounted on two horizontal tungsten wires (100 μm diameter) connected to a force displacement transducer and a movable device, respectively, in 5 ml organ bath of a small vessel myograph (MTOB-1, LaboSupport, Osaka, Japan). The organ bath was filled with normal physiological salt solution (Karaki et al., 1991) of the following composition (mM): NaCl 136.9, KCl 5.4, $CaCl_2$ 1.5, $MgCl_2$ 1.0, $NaHCO_3$ 23.8, glucose 5.5 and ethylenediamine tetraacetic acid 0.01. The solution was maintained at 37 ± 0.5. °C, and aerated with 95% O_2–5% CO_2, which maintained a pH of ~ 7.4. The preparations were equili-

* Corresponding author. Tel.: +81-96-373-5081; fax: +81-96-373-5082.
E-mail address: tokutomi@gpo.kumamoto-u.ac.jp (N. Tokutomi).

0014-2999/$ - see front matter © 2003 Elsevier B.V. All rights reserved.
doi:10.1016/S0014-2999(03)02128-9

brated for 60 min under 0.5 g of passive tension with rinsing every 15 min, and repeatedly exposed to phenylephrine (0.1 μM) until responses became stable. The isometric tension was monitored on a pen recorder (FBR-251A, Shimadzu, Japan) and stored on a digital data recorder (VR-10B, Instrutech, New York, USA).

Endothelium was present in all experiments except when indicated. For experiments with denuded aortic rings, the endothelium was removed by gently rubbing the luminal surface of the aortic rings with a stainless-steel rod. The endothelial function was assessed by testing the relaxatory effect of acetylcholine (1 μM) in the aortic rings precontracted with phenylephrine (0.1 μM). All peak relaxations to acetylcholine and α_1-acid glycoprotein were measured as percent reversal of the maximal phenylephrine-induced contraction prior to application of each relaxatory agent. The organ bath solution, containing high concentration (60 mM) of K^+, was prepared by replacing NaCl with equimolar KCl in normal solution. In the experiments with extracellular Ca^{2+} concentration of 10 mM, a 1 M stock solution of $CaCl_2$ was added directly to the organ bath.

Human α_1-acid glycoprotein (purified from Cohn Fraction VI) and L-phenylephrine were purchased from Sigma (St. Louis, MO). Acetylcholine, N^G-nitro-L-arginine methyl ester (L-NAME), N^G-monomethyl-L-arginine (L-NMMA) and heparin were from Wako (Osaka, Japan).

Experimental data are given as mean ± S.E.M., and the statistical significance was estimated by Student's *t*-test for comparisons between two groups and analysis of variance (ANOVA) with Dunnett's test for multiple comparisons. Differences were considered significant at $P<0.05$.

3. Results

3.1. Concentration-dependent relaxation with α_1-acid glycoprotein

Since the plasma level of α_1-acid glycoprotein is known to increase up to about 75 μM during acute phase reactions (Kremer et al., 1988), we tested the effects of human α_1-acid glycoprotein at 7.5–75 μM on isometric tension of isolated mouse aortic rings. Fig. 1A is a set of representative traces, showing the effects of α_1-acid glycoprotein on the tension of the endothelium-intact aorta precontracted with phenylephrine at 0.1 μM. α_1-Acid glycoprotein produced transient relaxations in a concentration-dependent manner. The concentration–response relation for the α_1-acid glycoprotein-induced relaxation is shown in Fig. 1B.

In 4 out of 36 aortic rings, the 75 μM α_1-acid glycoprotein-induced relaxation was followed by augmented contraction (see Fig. 2A), while the rest of rings tested revealed only relaxation. The augmentation in contraction was 5–13% of amplitude of the tonic precontraction before application of α_1-acid glycoprotein, although the values varied from ring to ring of aorta.

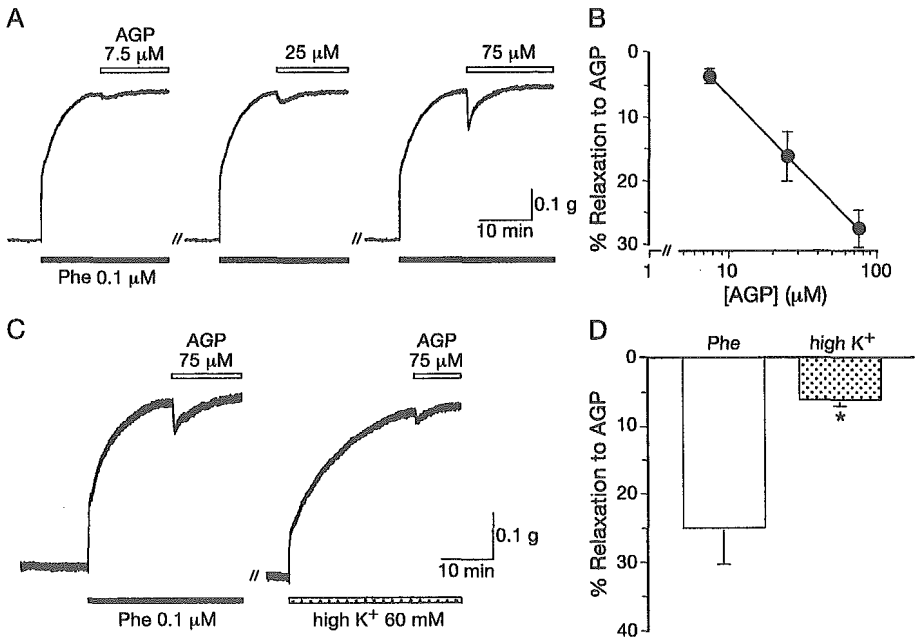

Fig. 1. (A) Concentration-dependent relaxation with α_1-acid glycoprotein. Representative traces showing the α_1-acid glycoprotein-induced relaxation at indicated concentrations in phenylephrine (0.1 μM)-precontracted rings of mouse aorta. AGP: α_1-acid glycoprotein. Phe: phenylephrine. (B) Average concentration–relaxation curves to α_1-acid glycoprotein from experiments as depicted in A. The relaxations are expressed in percent reversal of the maximal phenylephrine-induced contraction prior to application of α_1-acid glycoprotein. $N=8–28$. (C) Representative traces showing the α_1-acid glycoprotein-induced relaxation in phenylephrine- and high K^+ (60 mM)-precontracted aorta. (D) Average relaxations to α_1-acid glycoprotein (75 μM) in the phenylephrine-precontracted (open column) and high K^+-precontracted (dotted column) aorta from experiments as depicted in C. Values are expressed as percent reversal of the maximal phenylephrine-induced contraction prior to application of α_1-acid glycoprotein. $^*P<0.05$ vs. control.

α_1-Acid glycoprotein at 75 μM produced neither relaxation nor contraction when applied alone to the aortic rings at basal tone without any contractile stimulants ($n=5$). Human serum albumin (Fraction V) at 75 μM revealed neither relaxation nor contraction in all aortic rings tested ($n=5$) in the absence and presence of phenylephrine (data not shown).

3.2. Comparison of the effects of α_1-acid glycoprotein in phenylephrine- and high K^+-precontraction

It is important to know whether the α_1-acid glycoprotein-induced relaxation depends upon the mode of precontraction. We tested the effects of α_1-acid glycoprotein in aortic rings precontracted with a high K^+ (60 mM) external solution and compared the effects with those in phenylephrine-precontraction. As shown in Fig. 1C, α_1-acid glycoprotein elicited relaxations to smaller extent in the aortic rings precontracted with high K^+ solution than those with phenylephrine (5.9 ± 1.1% vs. 24.7 ± 5.4%, $n=8$, $P<0.05$; Fig. 1D). These results suggest that α_1-acid glycoprotein preferentially inhibit the phenylephrine-induced contraction.

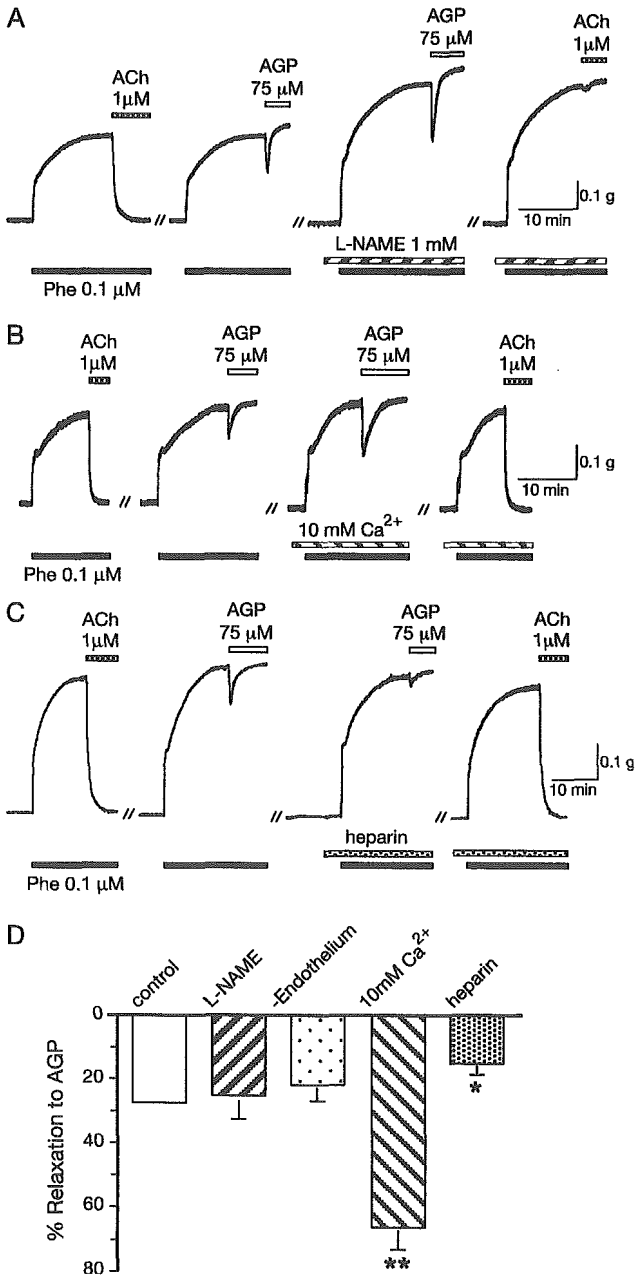

3.3. Involvement of nitric oxide-dependent pathways in α_1-acid glycoprotein-induced relaxation

To determine whether the vasorelaxant effect of α_1-acid glycoprotein involves nitric oxide (NO)-dependent pathways, we tested the effects of α_1-acid glycoprotein in the aortic rings treated with a NO synthase inhibitor, N^G-nitro-L-arginine methyl ester (L-NAME) and in the aortic rings of which the endothelia were removed. When L-NAME at 1 mM, which is the concentration that prevented the relaxations to acetylcholine at 1 μM, was administered to the aortic rings prior to application of phenylephrine, the α_1-acid glycoprotein-induced relaxation was rarely affected (25.1 ± 7.8%, $n=9$, vs. 27.6 ± 2.9% in controls; Fig. 2A and D). Similarly, N^G-monomethyl-L-arginine (L-NMMA, 0.1 mM) did not affect the α_1-acid glycoprotein-induced relaxation (data not shown). Consistently, removal of the endothelium revealed no significant change in the α_1-acid glycoprotein-induced relaxation (22.1 ± 5.3%, $n=8$; Fig. 2D).

3.4. Effects of increased extracellular calcium on α_1-acid glycoprotein-induced relaxation

It is known that mammalian oligosaccharides bearing sialic acid and fucose, such as sialyl-Lewis X (sLe^X), are parts of the functional carbohydrate moiety of α_1-acid

Fig. 2. (A) Involvement of NO-dependent pathways in the α_1-acid glycoprotein-induced relaxation. Representative traces showing the acetylcholine- or α_1-acid glycoprotein-induced relaxation in phenylephrine-precontracted aorta in the absence and presence of N^G-nitro-L-arginine methyl ester. AGP: α_1-acid glycoprotein. ACh: acetylcholine. Phe: phenylephrine. L-NAME: N^G-nitro-L-arginine methyl ester. (B) Effects of increased extracellular Ca^{2+} on the α_1-acid glycoprotein-induced relaxation. Representative traces showing the acetylcholine- or α_1-acid glycoprotein-induced relaxation in phenylephrine-precontracted aorta in control (1.5 mM) and high concentrations (10 mM) of extracellular Ca^{2+}. (C) Effects of heparin on the α_1-acid glycoprotein-induced relaxation. Representative traces showing the acetylcholine- or α_1-acid glycoprotein-induced relaxation in phenylephrine-precontracted aorta in the absence and presence of heparin (100 U/ml). (D) Average relaxations to α_1-acid glycoprotein (75 μM) in the phenylephrine-precontracted aorta under control (open column), N^G-nitro-L-arginine methyl ester-treated (hatched column) and endothelium-removed (dotted column) conditions, in high concentration of extracellular Ca^{2+} (hatched column), and under heparin-treated conditions (dotted column). Values are expressed as percent reversal of the maximal phenylephrine-induced contraction prior to application of α_1-acid glycoprotein. *$P<0.05$ and **$P<0.01$ vs. control.

glycoprotein (Bennett and Schmid, 1980) and are recognized by selectin family of cell adhesion molecules in a Ca^{2+}-dependent manner (Geng et al., 1990). To determine whether the vasorelaxant effects of α_1-acid glycoprotein in mouse aorta are Ca^{2+}-dependent, we compared the effects of α_1-acid glycoprotein in normal (1.5 mM) and high (10 mM) Ca^{2+}-containing external solutions. When extracellular Ca^{2+} concentration was raised to 10 mM, the α_1-acid glycoprotein-induced relaxation was potentiated in all phenylephrine-precontracted aortic rings tested ($66.6 \pm 6.7\%$, $n=8$, $P<0.01$; Fig. 2B and D). The α_1-acid glycoprotein-induced relaxation immediately recovered to the control level when extracellular Ca^{2+} concentration was returned to the normal level.

In contrast to those effects of elevated Ca^{2+} on the α_1-acid glycoprotein-induced relaxation, monovalent cations did not seem to be important modulators of the α_1-acid glycoprotein action, since the α_1-acid glycoprotein-induced relaxation was rarely affected when extracellular $Na^+$was replaced by Li^+ (data not shown).

3.5. Effects of heparin on α_1-acid glycoprotein-induced relaxation

We tested the effects of unfractionated heparin (100 U/ml) on the vasorelaxation induced by α_1-acid glycoprotein (Fig. 2C), since heparin is known to inhibit selectin binding to sLe^X in a Ca^{2+}-dependent manner (Nelson et al., 1993; Koenig et al., 1998). Heparin applied alone at concentrations up to 100 U/ml produced neither contraction nor relaxation in all aortic rings tested ($n=8$). Heparin also did not influence the phenylephrine-precontraction. Pretreatment of the aortic rings with heparin prior to application of phenylephrine resulted in a decrease in the α_1-acid glycoprotein-induced relaxation ($15.2 \pm 3.7\%$, $n=8$, $P<0.05$; Fig. 2D). This indicates that heparin (100 U/ml) was able to inhibit the relaxant effect of α_1-acid glycoprotein by 45%. The inhibitory effect of heparin on the α_1-acid glycoprotein-induced relaxation was immediately recovered when heparin was removed ($n=8$). These results suggest that the α_1-acid glycoprotein-induced relaxation may involve heparin-sensitive intermolecular interaction between α_1-acid glycoprotein and its binding sites on the vascular smooth muscle cells.

4. Discussion

In the present study, we have demonstrated that human α_1-acid glycoprotein produces a transient, concentration-dependent relaxation in the phenylephrine-precontracted aortic rings (Fig. 1). The transient relaxation with α_1-acid glycoprotein was rarely affected by L-NAME, L-NMMA, or removal of endothelium (Fig. 2), suggesting that production of endothelial NO does not play crucial roles in the development of the α_1-acid glycoprotein-induced relaxation. It is likely that α_1-acid glycoprotein acts more effectively at the stage of contraction, at which the contractility is governed by activation of α_1-adrenoceptor rather than voltage-dependent Ca^{2+} channels (VDCCs) on the vascular smooth muscle cells, as shown in Fig. 1C. α_1-Adrenoceptor activation in vascular smooth muscle cells is known to increase the intracellular free Ca^{2+} level by both inositol trisphosphate-dependent Ca^{2+} release and Ca^{2+} entry through nonselective cation channels (NSCCs) (Karaki et al., 1997). It is suggested that the α_1-acid glycoprotein-induced relaxation is achieved by inhibition of both VDCCs and NSCCs to a distinct extent in the smooth muscle cells.

The augmented contraction following the α_1-acid glycoprotein (75 μM)-induced relaxation, which was observed in 4 out of 36 aortic rings, might involve another source of Ca^{2+}, such as capacitative Ca^{2+} entry (Karaki et al., 1997), during blockade of VDCCs and NSCCs with α_1-acid glycoprotein, although the augmentation in contraction could not be evaluated quantitatively because of large variance of the extent of augmentation and its low rate of occurrence.

The potentiated relaxation with α_1-acid glycoprotein at high concentrations of extracellular Ca^{2+} (10 mM) may inform us about the selective recognition by its binding sites on the vascular smooth muscle cells, since the α_1-acid glycoprotein-induced relaxation was rarely affected when extracellular $Na^+$was replaced by Li^+. The immediate recovery from the potentiation of α_1-acid glycoprotein-induced relaxation by washing out the high Ca^{2+}-containing external solution with the normal external solution may favor the external site of action for the Ca^{2+}-dependent potentiation of the α_1-acid glycoprotein-induced relaxation. The effects of extracellular Ca^{2+} on the α_1-acid glycoprotein-induced relaxation might be due to the Ca^{2+}-dependent recognition of the carbohydrate moiety of α_1-acid glycoprotein by selectin family (Bennett and Schmid, 1980; Geng et al., 1990).

It has been reported that heparin fragments as small as tetrasaccharides specifically block the interactions of selectin with sLe^X-containing ligands (Nelson et al., 1993; Koenig et al., 1998). Heparin is also known to inhibit inositol trisphosphate-dependent Ca^{2+} release from the sarcoplasmic reticulum when applied intracellularly. Our results show that the α_1-acid glycoprotein-induced relaxation was moderately, but significantly, inhibited in the presence of heparin and that the inhibition of the relaxation was immediately recovered by removal of heparin. The immediate recovery of the α_1-acid glycoprotein-induced relaxation suggested that the action of heparin occurs extracellularly. The functional lectin-like domain which may interact with sLe^X moieties on α_1-acid glycoprotein might be expressed at the surface of vascular smooth muscle cells and heparin might inhibit the interaction of the lectin-like domain with sLe^X on α_1-acid glycoprotein.

In conclusion, we have demonstrated that human α_1-acid glycoprotein produces a transient relaxation in the mouse aorta precontracted with phenylephrine. It is more likely that the α_1-acid glycoprotein-induced relaxation is due to block of Ca^{2+} entry through VDCC or NSCC in the smooth

muscle cells rather than activation of endothelial NO pathway. The interaction between α_1-acid glycoprotein molecules and plasmalemmal Ca^{2+} entry channels may be modified by extracellular Ca^{2+} and heparin.

The physiological significance of the α_1-acid glycoprotein-induced transient relaxation of mouse aorta is at present a matter for speculation. The transient relaxation induced by α_1-acid glycoprotein might occur as prolonged relaxation in the peripheral blood vessel, which may result in improvement of the blood circulation in tissues with inflammation. Testing additional biological parameters, further investigations are needed to fully illustrate the physiological roles of α_1-acid glycoprotein.

Acknowledgements

This study was supported in part by grants-in-aid for scientific research from the Ministry of Education, Science, Sports and Culture of Japan.

References

Bennett, M., Schmid, K., 1980. Immunosuppression by human plasma alpha 1-acid glycoprotein: importance of the carbohydrate moiety. Proc. Natl. Acad. Sci. U. S. A. 77, 6109–6113.

Fournier, T., Medjoubi-N, N., Porquet, D., 2000. Alpha-1-acid glycoprotein. Biochim. Biophys. Acta 1482, 157–171.

Geng, J.-G., Bevilacqua, M.P., Moore, K.L., McIntyre, T.M., Prescott, S.M., Kim, J.M., Bliss, G.A., Zimmerman, G.A., McEver, R.P., 1990. Rapid neutrophil adhesion to activated endothelium mediated by GMP-140. Nature 343, 757–760.

Karaki, H., Ozaki, H., Hori, M., Mitsui-Saito, M., Amano, K., Harada, K., Miyamoto, S., Nakazawa, H., Won, K.-J., Sato, K., 1997. Calcium movements, distribution, and functions in smooth muscle. Pharmacol. Rev. 49, 157–230.

Karaki, H., Sato, K., Ozaki, H., 1991. Different effects of verapamil on cytosolic Ca^{2+} and contraction in norepinephrine-stimulated vascular smooth muscle. Jpn. J. Pharmacol. 55, 35–42.

Koenig, A., Norgard-Sumnicht, K., Linhardt, R., Varki, A., 1998. Differential interactions of heparin and heparan sulfate glycosaminoglycans with the selectins. Implications for the use of unfractionated and low molecular weight heparins as therapeutic agents. J. Clin. Invest. 101, 877–889.

Kremer, J.M., Wilting, J., Janssen, L.H., 1988. Drug binding to human alpha-1-acid glycoprotein in health and disease. Pharmacol. Rev. 40, 1–47.

Maeda, H., Nishi, K., Mori, I., 1980. Facilitating effects of alpha-1 acid glycoprotein on the passage of erythrocytes through the membrane-filter. Life Sci. 27, 157–161.

Nelson, R.M., Cecconi, O., Roberts, W.G., Aruffo, A., Linhardt, R.J., Bevilacqua, M.P., 1993. Heparin oligosaccharides bind L- and P-selectin and inhibit acute inflammation. Blood 82, 3253–3258.

Sorensson, J., Matejka, G.L., Ohlson, M., Haraldsson, B., 1999. Human endothelial cells produce orosomucoid, an important component of the capillary barrier. Am. J. Physiol. 276, H530–H534.

Journal of Enzyme Inhibition and Medicinal Chemistry, 2003 VOL. 18 (1), pp. 35–39

Taylor&Francis
healthsciences

Inactivation of Rabbit Liver Carbonyl Reductase by Phenylglyoxal and 2,3,4-Trinitrobenzenesulfonate Sodium

YORISHIGE IMAMURA[a,*], TOSHIHISA KOGA[a], HIDEAKI SHIMADA[b] and MASAKI OTAGIRI[a]

[a]*Faculty of Pharmaceutical Sciences, Kumamoto University, 5-1, Oe-honmachi Kumamoto 862-0973, Japan;* [b]*Faculty of Education, Kumamoto University, 2-40-1, Kurokami, Kumamoto 860-8555, Japan*

(Received 28 August 2000)

The chemical modifications of rabbit liver carbonyl reductase (RLCR) with phenylglyoxal (PGO) and 2,3,4-trinitrobenzenesulfonate sodium (TNBS), which are respective chemical modifiers of arginine and lysine residues, were examined. RLCR was rapidly inactivated by these modifiers. Kinetic data for the inactivation demonstrated that each one of arginine and lysine residues is essential for catalytic activity of the enzyme. Furthermore, based on the protective effects of $NADP^+$, NAD^+ and their constituents against the inactivation of RLCR by PGO and TNBS, we propose the possibility that the functional arginine and lysine residues are located in the coenzyme-binding domain of RLCR and interact with the 2′-phosphate group of NADPH.

Keywords: Carbonyl reductase; Chemical modification; Rabbit liver; Arginine residue; Lysine residue; Coenzyme-binding domain

INTRODUCTION

Carbonyl reductase (EC 1.1.1.184) is considered as a drug-metabolizing enzyme catalyzing the ketone-reduction of drugs such as acetohexamide, befunolol and daunorubicin.[1–3] A variety of carbonyl reductases have been purified from the liver, kidney, lung, brain and heart of mammalian species.[4–10] We have purified a carbonyl reductase from the cytosolic fraction of rabbit liver, using befunolol as a substrate,[11] since the liver is most important organ in the metabolism of drugs. As expected, the purified rabbit liver carbonyl reductase (RLCR) had the ability to effectively reduce ketone-containing drugs.[11]

It has been reported that several NADPH-dependent enzymes including carbonyl reductase have arginine and lysine residues located in their coenzyme-binding domain.[12–15] These amino acid residues have been demonstrated to serve a principal role in the binding and specificity of coenzyme. For example, NADPH-dependent aldehyde reductase purified from pig kidney has functional arginine and lysine residues in its coenzyme-binding domain.[12,16] Furthermore, our work[17] has revealed that indomethacin, a nonsteroidal anti-inflammatory drug, interacts with or near one essential arginine residue located in the coenzyme-binding domain of rabbit kidney carbonyl reductase. It is possible that nonsteroidal anti-inflammatory drugs inhibit carbonyl reductases, by interacting with an arginine or lysine residue located in the coenzyme-binding domain. The purpose of the present study is to elucidate that the functional amino acid residue is located in the coenzyme-binding domain of RLCR, as well as rabbit kidney carbonyl reductase. Consequently we attempted the inactivation of RLCR by phenylglyoxal (PGO) and 2,3,4-trinitrobenzenesulfonate sodium (TNBS), which are respective chemical modifiers of arginine and lysine residues. The protective effects of $NADP^+$, NAD^+ and their constituents against the inactivation of RLCR by PGO and TNBS were also examined.

MATERIALS AND METHODS

Materials

Carbonyl reductase was purified from the cytosolic fraction of rabbit liver as described previously.[11] Acetohexamide used as the substrate was obtained

*Corresponding author. E-mail: yorishig@gpo.kumamoto-u.ac.jp

ISSN 1475-6366 print/ISSN 1475-6374 online © 2003 Taylor & Francis Ltd
DOI: 10.1080/1475636021000049203

from Shionogi (Osaka, Japan). The purified enzyme (rabbit liver carbonyl reductase, RLCR) was a homogeneous protein on sodium dodecyl sulfate (SDS)-polyacrylamide gel electrophoresis. Befunolol (Kaken Pharmaceutical, Tokyo, Japan), loxoprofen (Sankyo, Tokyo, Japan) and daunorubicin (Meiji Seika, Tokyo, Japan) were provided by the manufacturers. PGO, TNBS and 4-acetylpyridine (4-AP) were purchased from Tokyo Kasei Kogyo (Tokyo, Japan). 2′-AMP, 5′-AMP, 5′-ADP, 2′,5′-ADP, 2′-phospho-5′-ADP-ribose, nicotinamide mononucleotide (NMN) and NAD^+ were obtained from Sigma (St. Louis, MO, USA). NADPH and $NADP^+$ were products from Oriental Yeast (Tokyo, Japan). All other chemicals were of reagent grade.

Enzyme Assay

RLCR activity was assayed spectrophotometrically by monitoring NADPH oxidation at 340 nm. The reaction mixture in a total volume of 0.7 ml consisted of 0.1 M sodium potassium phosphate buffer (pH 6.5), 0.25 mM NADPH, substrate at various concentrations and the purified enzyme. The reaction was initiated by adding the enzyme sample, and the decrease in absorbance at 340 nm was monitored with a Shimadzu UV-240 spectrophotometer. One unit of enzyme activity was defined as the amount catalyzing the oxidation of 1 μmole/min of NADPH at 30°C. Protein concentration was determined by the method of Lowry *et al.*[18] using bovine serum albumin as the standard. The K_m and V_{max} values of the enzyme for ketone-containing drugs were calculated using a computer program for least-squares linear regression of double-reciprocal plots.

Chemical Modification

After pre-incubation for 3 min, the enzyme (4.2–6.6 μM) was incubated with PGO (2.5–10 mM) or TNBS (0.25–2.0 mM) in 0.1 M sodium potassium phosphate buffer (pH 7.4) at 30°C. In the case of modification with TNBS, the reaction mixture was kept in the dark. Aliquots (10–20 μl) were withdrawn at appropriate intervals and diluted, then the enzyme activities were assayed using 1.0 mM acetohexamide as the substrate. A control containing no modifier was routinely included and the residual activity (%) was calculated relative to the control.

RESULTS

Substrate Specificities of RLCR for Drugs having a Ketone Group

RLCR has been purified from cytosolic fraction of rabbit liver using befunolol as the substrate.[11] In this study, acetohexamide was used as a substrate instead of befunolol. Thus, we re-examined the substrate specificity of RLCR for drugs having a ketone group within their chemical structures. RLCR was confirmed to catalyze the ketone-reduction of various drugs such as befunolol, loxoprofen and daunorubicin including acetohexamide, and function as a drug-metabolizing enzyme (Table I).

Inactivation of RLCR by PGO

We investigated the chemical modification of RLCR with PGO, a typical chemical modifier of arginine residues. RLCR was rapidly inactivated by PGO and the inactivation reaction was time- and concentration-dependent (Figure 1A). The secondary plots of the pseudo-first-order rate constants *versus* the concentrations of PGO gave a straight line through the origin (Figure 1B), indicating that the modification is the result of a simple bimolecular reaction, in which a reversible PGO-enzyme complex is not formed before inactivation. Furthermore, a straight line with a slope of 1.1 was obtained from the double logarithmic plots according to the method of Levy *et al.*[19] (Figure 1C). This implies that 1 mol of the enzyme is inactivated by 1 mol of PGO, that is, that one arginine residue is essential for the enzyme activity.

Inactivation of RLCR by TNBS

The chemical modification of RLCR with TNBS, a typical chemical modifier of lysine residues, also caused time- and concentration-dependent loss of the enzyme activity, as shown in Figure 2A. Kinetic data for the inactivation were similar to those obtained in the inactivation of RLCR by PGO (Figures 2B and 2C), indicating that one lysine residue is essential for the enzyme activity.

Protective Effects of $NADP^+$ and 4-Acetylpyridine (4-AP) against the Inactivation of RLCR by PGO and TNBS

The protective effects of $NADP^+$ (coenzyme) and 4-AP (substrate) against the inactivation of RLCR by PGO were examined. $NADP^+$ was used as a coenzyme instead of NADPH, because PGO is

TABLE I Substrate specificity of RLCR for ketone-containing drugs

Drugs	K_m (mM)	V_{max} (units/mg)
Acetohexamide	0.92	3.39
Befunolol	1.44	4.08
Loxoprofen	0.52	1.06
Daunorubicin	3.00	41.0

The values are the means of at least two experiments.

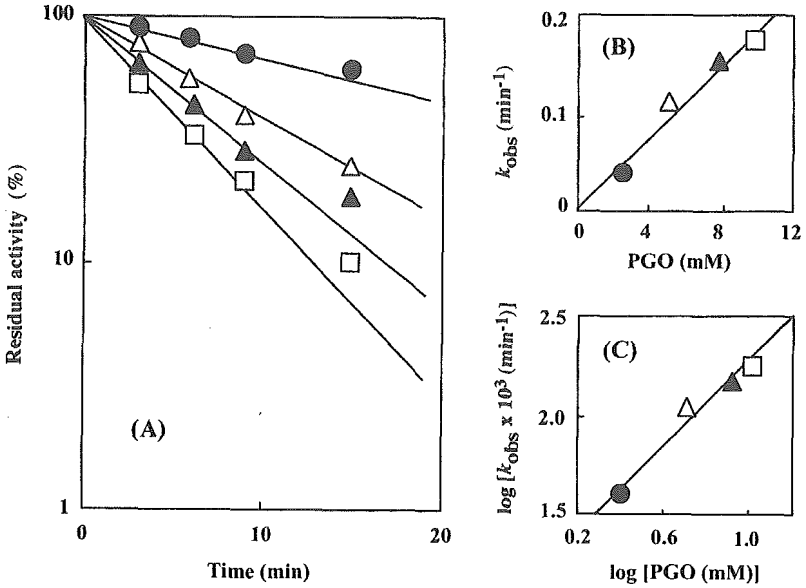

FIGURE 1 Inactivation of RLCR by PGO. (A) The enzyme was incubated with 2.5 mM (●), 5.0 mM (△), 7.5 mM(▲) and 10 mM (□) PGO. (B) Secondary plots of the pseudo-first-order constant (k_{obs}) versus the concentration of PGO. (C) Double logarithmic plots for the determination of the order of the inactivation reaction.

a substrate for the enzyme in the presence of NADPH. Our work has revealed that the enzyme reaction follows an ordered Bi–Bi mechanism, in which NADPH binds to the enzyme first and $NADP^+$ leaves last.[20] Thus, if the essential amino acid residue is located in the coenzyme-binding domain, the inactivation of RLCR by PGO will be protected in the presence of only $NADP^+$. Whereas if the essential amino acid residue is located in the substrate-binding domain, the inactivation of RLCR by PGO will be protected in the presence of both $NADP^+$ and 4-AP. As shown in Figure 3, the protective effect against the inactivation was observed in the presence of only $NADP^+$, but was unaffected by the addition of 4-AP. These results indicate that one essential arginine residue is located in the coenzyme-binding domain. Similar protective effects were found against the inactivation of the enzyme by TNBS (data not shown), indicating the presence of one essential lysine residue located in coenzyme-binding domain.

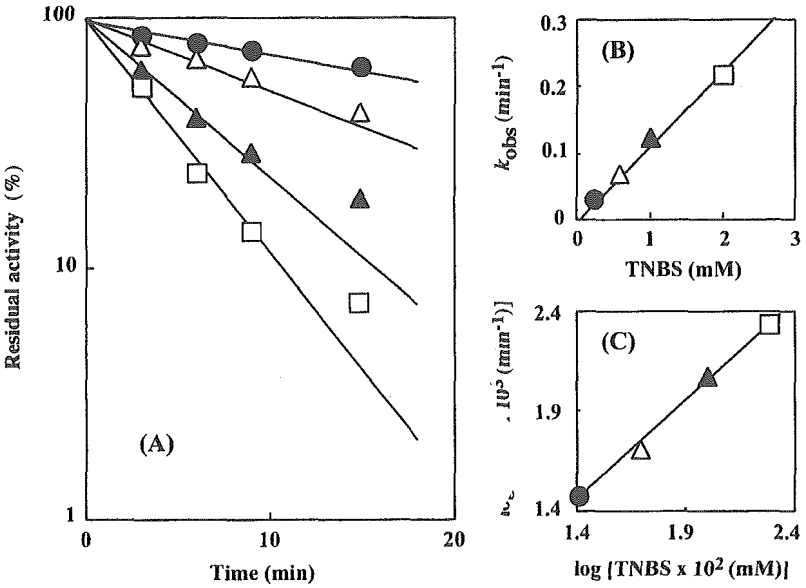

FIGURE 2 Inactivation of RLCR by TNBS. (A) The enzyme was incubated with 0.25 mM (●), 0.5 mM (△), 1.0 mM (▲) and 2.0 mM (□) TNBS. (B) Secondary plots of the pseudo-first-order constant (k_{obs}) versus the concentration of TNBS. (C) Double logarithmic plots for the determination of the order of the inactivation reaction.

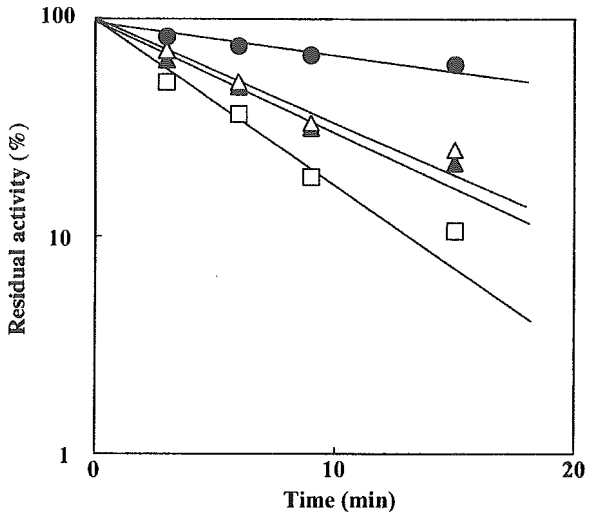

FIGURE 3 Protective effects of $NADP^+$ and substrate 4-AP against the inactivation of RLCR by PGO. The enzyme was incubated with 10 mM PGO (□), 10 mM PGO + 1 μM $NADP^+$ (▲), 10 mM PGO + 1 μM $NADP^+$ + 1.0 mM 4-AP (△) and 10 mM PGO + 5 μM $NADP^+$ (●).

Protective Effects of $NADP^+$, NAD^+ and their Constituents against the Inactivation of RLCR by PGO and TNBS

Table II summarizes the protective effects of $NADP^+$, NAD^+ and their constituents against the inactivation of RLCR by PGO and TNBS. The half-life ($t_{1/2}$) was estimated from the apparent pseudo-first-order rate constant. As described above, $NADP^+$ effectively protected the inactivation of the enzyme by PGO and TNBS, but NAD^+ did not. 2′-AMP, 2′,5′-ADP and 2′-phospho-5′-ADP-ribose afforded protective effects against the inactivation of the enzyme by PGO and TNBS, whereas 5′-AMP, 5′-ADP or NMN, which lack a 2′-phosphate group, were without effect. The results suggest that the functional arginine and lysine residues located in the coenzyme-binding domain of RLCR interact with the 2′-phosphate group of NADPH.

DISCUSSION

Kinetic data for the inactivation of RLCR by PGO and TNBS provide evidence that each one of the arginine and lysine residues is essential for the enzyme activity. Furthermore, this study demonstrates that the functional arginine and lysine residues are located in the coenzyme-binding domain of RLCR, based on the protective effect of $NADP^+$ against the inactivation of RLCR by PGO and TNBS.

Sciotti and Wermuth[15] have shown the importance of arginine and lysine residues at positions of 38 and 15, respectively, for NADPH binding in human carbonyl reductase. The mutant enzyme R38Q (substitution of Gln for Arg-38 of human carbonyl reductase) exhibits a significant enzyme activity. Interestingly, R38Q is inactivated by PGO to the same extent as the native enzyme, suggesting that, in addition to Arg-38, at least one other arginine residue contributes to the binding of NADPH. As is evident from Figure 4, the amino acid sequence deduced from the RLCR gene (*RCBR5*) has a high identity with that of human carbonyl reductase.[21,22] However, in the amino acid sequence of RLCR, position 38, unlike that of human carbonyl reductase, is Gln. One essential arginine residue of RLCR probably corresponds to an arginine residue other than position 38 responsible for NADPH binding in human carbonyl reductase, although the position number in the amino acid sequence remains to be determined.

The limited data for the protective effects of $NADP^+$, NAD^+ and their constituents against the inactivation of RLCR by PGO and TNBS lead us to suggest that arginine and lysine residues serve as positively charged sites and interact with the 2′-phosphate group of NADPH. Similar results are observed for arginine and lysine residues in the coenzyme-domain of enzymes belonging to the families of aldo–keto reductase and short-chain dehydrogenase/reductase (SDR): aldose and aldehyde reductases, and carbonyl reductase are members of aldo-keto reductases and SDRs, respectively.[23,24] For example, crystallographic analysis of recombinant human placenta aldose reductase complexed with NADPH reveals that Arg-268 and Lys-262 residues are involved in the interaction with the 2′-phosphate group of NADPH.[25] Two basic residues, Arg-39 and Lys-17, in mouse tetrameric carbonyl reductase also promote NADPH binding by interacting with the 2′-phosphate group.[14,26] It is reasonable to assume that arginine and lysine residues located in the coenzyme-binding domain of aldo-keto reductases and SDRs play a role in the binding and specificity of coenzyme.

TABLE II Protective effects of $NADP^+$, NAD^+ and their constituents against the inactivation of RLCR by PGO and TNBS

	$t_{1/2}$ (min)	
Coenzyme (concentration)	PGO	TNBS
Control	4	3
$NADP^+$ (5 μM)	48	39
NAD^+ (1 mM)	4	4
2′-AMP (1 mM)	12	10
5′-AMP (1 mM)	4	3
5′-ADP (1 mM)	4	4
2′,5′-ADP (1 mM)	12	31
2′-phospho-5′-ADP-ribose (1 mM)	21	48
NMN (1 mM)	5	3

The enzyme was incubated with 10 mM PGO or 2.0 mM TNBS. The values are the means of at least two experiments.

```
                                        *
HCR   MSSGIHVALVTGGNKGIGLAIVRDLCRLFSGDVVLTARDVTRGQAAVQQL   50
RLCR  MPSDRRVALVTGANKGVGFAITRALCRLFSGDVLLTAQDEAQGQAAVQQL   50

HCR   QAEGLSPRFHQLDIDDLQSIRALRDFLRKEYGGLDVLVNNAGIAFKVADP  100
RLCR  QAEGLSPRFHQLDITDLQSIRALRDFLRRAYGGLNVLVNNAVIAFKMEDT  100

HCR   TPFHIQAEVTMKTNFFGTRDVCTELLPLIKPQGRVVNVSSIMSVRALKSC  150
RLCR  TPFHIQAEVTMKTNFDGTRDVCTELLPLMRPGGRVVNVSSMTCLRALKSC  150

HCR   SPELQQKFRSETITEEELVGLMNKFVEDTKKGVHQKEGWPSSAYGVTKIG  200
RLCR  SPELQQKFRSETITEEELVGLMKKFVEDTKKGVHQTEGWPDTAYGVTKMG  200

HCR   VTVLSRIHARKLSEQRKGDKILLNACCPGWVRTDMAGPKATKSPEEGAET  250
RLCR  VTVLSRIQARHLSEHRGGDKILVNACCPGWVRTDMGGPNATKSPEEGAET  250

HCR   PVYLALLPPDAEGPHGQFVSEKRVEQW                         277
RLCR  PVYLALLPPDAEGPHGQFVMDKKVEQW                         277
```

FIGURE 4 Amino acid sequences of RLCR and human carbonyl reductase (HCR). The sequence data were cited from references 21 and 22. Asterisk shows Arg-38 of HCR.

It has been reported that nonsteroidal anti-inflammatory drugs including indomethacin are potent inhibitors of carbonyl reductases.[27,28] RLCR is also known to be inhibited by a variety of nonsteroidal anti-inflammatory drugs.[29] Further studies are in progress to elucidate whether or not nonsteroidal anti-inflammatory drugs interact with the functional arginine and lysine residues located in the coenzyme-binding domain of RLCR.

References

[1] Jakoby, W.B. and Ziegler, D.M. (1990) *J. Biol. Chem.* **265**, 20715–20718.
[2] Oppermann, U.C.T. and Maser, E. (2000) *Toxicology* **144**, 71–90.
[3] Forrest, G.L. and Gonzalez, B. (2000) *Chem.-Biol. Interact.* **129**, 21–40.
[4] Sawada, H., Hara, A., Nakayama, T. and Kato, F. (1980) *J. Biochem. (Tokyo)* **87**, 1153–1165.
[5] Ikeda, M., Hattori, H. and Ohmori, S. (1984) *Biochem. Pharmacol.* **33**, 3957–3961.
[6] Hara, A., Nakayama, T., Deyashiki, Y., Kariya, K. and Sawada, H. (1986) *Arch. Biochem. Biophys.* **244**, 238–247.
[7] Imamura, Y., Higuchi, T., Nozaki, Y., Sugino, E., Hibino, S. and Otagiri, M. (1993) *Arch. Biochem. Biophys.* **300**, 570–576.
[8] Nakayama, T., Hara, A. and Sawada, H. (1982) *Arch. Biochem. Biophys.* **217**, 564–573.
[9] Wermuth, B. (1981) *J. Biol. Chem.* **256**, 1206–1213.
[10] Imamura, Y., Migita, T., Otagiri, M., Choshi, T. and Hibino, S. (1999) *J. Biochem. (Tokyo)* **125**, 41–47.
[11] Imamura, Y., Nozaki, Y. and Otagiri, M. (1989) *Chem. Pharm. Bull.* **37**, 3338–3342.
[12] Davidoson, W.S. and Flynn, T.G. (1979) *J. Biol. Chem.* **254**, 3724–3729.
[13] Bohren, K.M., von Wartburg, J.P. and Weumuth, B. (1987) *Biochim. Biophys. Acta* **916**, 185–192.
[14] Tanaka, N., Nonaka, T., Nakanishi, M., Deyashiki, Y., Hara, A. and Mitsui, Y. (1996) *Structure* **4**, 33–45.
[15] Sciotti, M.A. and Wermuth, B. (2001) *Chem.-Biol. Interact.* **130–132**, 871–878.
[16] Flynn, T.G., Gallerneault, C., Ferguson, D., Cromlish, J.A. and Davidoson, W.S. (1981) *Biochem. Soc. Trans.* **9**, 273–275.
[17] Higuchi, T., Imamura, Y. and Otagiri, M. (1994) *Biochim. Biophys. Acta* **1199**, 81–86.
[18] Lowry, O.H., Rosebrough, N.J., Farr, A.L. and Randall, R.J. (1951) *J. Biol. Chem.* **193**, 265–275.
[19] Levy, H.M., Leber, P.D. and Rayn, E.M. (1963) *J. Biol. Chem.* **238**, 3654–3659.
[20] Nozaki, Y., Imamura, Y. and Otagiri, M. (1990) *Chem. Pharm. Bull.* **38**, 156–158.
[21] Gonzalez, B., Sapra, A., Rivera, H., Kapolan, W.P., Yam, B. and Forrest, G.L. (1995) *Gene* **154**, 297–298.
[22] Wermuth, B., Bohren, K.M., Heinemann, G., von Wartburg, J.P. and Gabbay, K.H. (1988) *J. Biol. Chem.* **263**, 16185–16188.
[23] Bohren, K.M., Bullock, B., Wermuth, B. and Gabbay, K.H. (1989) *J. Biol. Chem.* **264**, 9547–9551.
[24] Jörnvall, H., Persson, B., Krook, M., Atrian, S., Gonzàlez-Duarte, R., Jeffery, J. and Ghosh, D. (1995) *Biochemistry* **34**, 6003–6013.
[25] Wilson, D.K., Bohren, K.M., Gabbay, K.H. and Quiocho, F.A. (1992) *Science* **257**, 81–84.
[26] Nakanishi, M., Kakumoto, M., Matsuura, K., Deyashiki, Y., Tanaka, N., Nonaka, T., Mitsui, Y. and Hara, A. (1996) *J. Biochem. (Tokyo)* **120**, 257–263.
[27] Higuchi, T., Imamura, Y. and Otagiri, M. (1994) *Biochem. Mol. Biol. Int.* **32**, 531–536.
[28] Terada, T., Niwase, N., Koyama, I., Imamura, M., Toya, H. and Mizoguchi, T. (1993) *Int. J. Biochem.* **25**, 1233–1239.
[29] Imamura, Y., Nozaki, Y., Higuchi, T. and Otagiri, M. (1991) *Res. Commun. Chem. Pathol. Pharmacol.* **71**, 49–57.

Pharmaceutical Research, Vol. 20, No. 4, April 2003 (© 2003) *Research Paper*

Validation of the Chloramine-T Induced Oxidation of Human Serum Albumin as a Model for Oxidative Damage *in Vivo*

Makoto Anraku,[1] Ulrich Kragh-Hansen,[2] Keiichi Kawai,[3] Toru Maruyama,[1] Yasuomi Yamasaki,[4] Yoshinobu Takakura,[4] and Masaki Otagiri[1,5]

Received September 11, 2002; accepted January 2, 2003.

Purpose. The validity of using chloramine-T as a model compound for mimicing oxidative stress was examined using human serum albumin (HSA) as a model. Important sites of oxidation were studied by mild treatment with chloramine-T and by mutating ^{34}Cys for a serine (C34S).

Methods. High-performance liquid chromatography (HPLC) combined with fluorescence detection to confirm the validity of chloramine-T as an oxidizing agent was used. Oxidized amino acid residues were detected by reaction with 5,5′-dithiobis(2-nitro benzoic acid), digestion with cyanogen bromide, followed by capillary electrophoresis. Protein conformation was examined by spectroscopic techniques.

Results. From the HPLC analysis of human serum, the validity of using chloramine-T as an oxidizing agent was confirmed. At low chloramine-T concentrations ($CT_{0.1}$-HSA, CT_1-HSA), ^{34}Cys and Met residues were oxidized, at medium concentrations (CT_{10}-HSA), the tryptophan residue also appeared to be oxidized, and at the highest concentration (CT_{50}-HSA), the net charge of Site II of HSA was found to be more negative. The two highest levels of oxidation of HSA (CT_{10}-HSA, CT_{50}-HSA) resulted in conformational changes with an increased exposure of hydrophobic regions, decreased high-affinity bindings of warfarin and ketoprofen and a reduced esterase-like activity. The latter protein also has a shorter plasma half-life and an increased liver clearance.

Conclusions. We succeeded in imitating oxidative damage to HSA using chloramine-T and the findings show that Site II is more affected than Site I and ^{34}Cys, when HSA is exposed to oxidative stress.

KEY WORDS: human serum albumin; cysteine mutation; chloramine-T; Site II; oxidative damage; pharmacokinetics.

INTRODUCTION

Covalent modification of proteins by oxidative systems has been implicated in various physiological and pathological conditions (1). To protect against this toxicity, organisms have developed a battery of antioxidant defenses. Thus, blood plasma, which is known to be exposed to continuous oxidative stress, contains albumin as a major and predominant circulating antioxidant (2). Human serum albumin (HSA) is a single, nonglycosylated polypeptide of 585 amino acids which is organized in the form of a heart-shaped protein having about 67% α-helix but no β-sheet structure (3). All but one (^{34}Cys) of the thirty-five cysteine (Cys) residues are involved in the formation of stabilizing disulfide bonds. Human serum albumin is also a comprehensive depot and transport protein, and plays an important role with respect to endogenous and exogenous compounds. Therefore, it can be anticipated that, for example, the distribution and half life of ligands might be greatly effected, if the functional properties of HSA were to be modified by disease or aging associated oxidation.

In a previous study, we oxidized HSA using several different procedures and found that several types of amino acid residues are important for its antioxidant activity (4). However, our experimental system was limited to *in vitro* conditions. Thus, it was difficult to judge whether our experimental conditions actually reflect physiological conditions. In a recent study, Era *et al.* (5) reported on the use of a convenient high-performance liquid chromatographic (HPLC) system for the clear separation of reduced and oxidized albumin, using an ES-502N column, and extensively studied the conversion of reduced; HSA to an oxidized form in the elderly and in various pathophysiological states. In general, HSA is a mixture of mercaptalbumin (HMA, reduced form) and nonmercapt albumin (HNA, oxidized form) (6,7). HMA contains one free sulfhydryl group in ^{34}Cys and HNA is comprised of at least three types of molecules, namely a mixed disulfide with cysteine or glutathione (HNA(Cys), HNA(Glut)), and products oxidized HNA (HNA(Oxi)) to a greater extent than mixed disulfide. The chloramine-T method of Shechter *et al.* (8) generates the formation of $HO^{\cdot}$ and chloro radicals and may mimic oxidation reactions that occur under physiological conditions. Preliminary results showed an increase in HNA, when reacting serum was reacted with chloramine-T. Similar results have been found in aging as well as in certain diseased states. Furthermore, by varying the experimental conditions, different types of HSA, in different oxidation states could be prepared easily and reproducibly. Therefore, we chose to further investigate this procedure for oxidizing HSA.

The authors also prepared a recombinant mutant of HSA in which ^{34}Cys was replaced by a serine, because ^{34}Cys represents a potentially important residue of HSA for oxidative stress. The impact of the mutation and four levels of chloramine-T induced oxidations on the structural properties of albumin was investigated using a variety of spectroscopic techniques. The influence of oxidation on various functional properties, namely its ligand-binding and esterase-like ability, were also studied. Finally, the effect of the mutation and oxidations on the plasma half-life and organ clearances of HSA was evaluated in mice.

[1] Faculty of Pharmaceutical Sciences, Kumamoto University, 5-1 Oe-honmachi, Kumamoto 862-0973, Japan.
[2] Department of Medical Biochemistry, University of Aarhus, DK-8000 Aarhus C, Denmark.
[3] School of Health Sciences, Faculty of Medicine, Kanazawa University, 5-11-80 Kodatsuno, Ishikawa 920, Japan.
[4] Department of Drug Delivery Research, Graduate School of Pharmaceutical Sciences, Kyoto University, Sakyo-ku 606-8501, Kyoto, Japan.
[5] To whom correspondence should be addressed. (e-mail: otagirim@gpo.kumamoto-u.ac.jp)-

ABBREVIATIONS: HSA, human serum albumin; rHSA, recombinant HSA; HMA, mercaptalbumin; HNA, nonmercaptalbumin; $CT_{0.1}$-HSA, CT_1-HSA, CT_{10}-HSA and CT_{50}-HSA is HSA treated with 0.1, 1, 10 and 50 mM of chloramine-T, respectively; DTNB, 5,5′-dithiobis (2-nitro benzoic acid); bis-ANS, 1,1-bis-4-anilinonaphthalene-5,5-sulfonic acid; CNBr, cyanogen bromide; CD, circular dichroism; Cys, cysteine; Met, methionine; Trp, tryptophan; Tyr, tyrosine.

0724-8741/03/0400-0684/0 © 2003 Plenum Publishing Corporation

Based on these data, the validity of chloramine-T treatment as a physiological model and the importance of Site I and Site II in HSA with respect to oxidative damage, are discussed.

MATERIALS AND METHODS

Materials

HSA was donated by the Chemo-Sera-Therapeutic Research Institute (Kumamoto, Japan) and was defatted by using the charcoal procedure described by Chen (9), deionized, freeze-dried, and then stored at −20°C until used. HSA and the oxidized HSAs prepared in this study gave only one band on SDS-PAGE (data not shown), and the molecular mass of all the albumins were assumed to be 67 kDa. Sera from five healthy young male subjects, who had no renal or hepatic dysfunctions, were obtained from Faculty of Pharmaceutical Sciences, Kumamoto University. Their ages ranged from 21 to 26 years (23.2 ± 1.92. mean ± S.D.), as previously described (10). Blood sera were obtained by centrifugation and stored at −80°C until used for analysis. Chloramine-T, 5,5′-dithiobis(2-nitro benzoic acid) (DTNB) and *p*-nitrophenyl acetate were purchased from Nacalai Tesque, Inc. (Kyoto, Japan). The fluorescence probe 1,1-bis-4-anilino-naphthalene-5,5-sulfonic acid (bis-ANS) and fluoresceinamine (isomer II) were obtained from Sigma (St Louis, MO, USA). Potassium warfarin (Eisai Co., Tokyo, Japan) and ketoprofen (Sanwakagaku Co., Tokyo, Japan) were obtained as pure substances from the manufacturers. $^{111}InCl_3$ (74 Mbq/mL in 0.02 N HCl) was a gift from Nihon Medi-Physics (Takarazuka, Japan). All other chemicals were of analytical grade, and all solutions were prepared in deionized and distilled water. Phosphate buffer, 67 mM and pH 7.4, was used as a standard buffer, and was prepared from sodium phosphate dibasic and sodium phosphate monobasic salts.

Synthesis and Purification of rHSA Forms

The recombinant DNA techniques used to produce wild-type rHSA and the single-residue mutant C34S were essentially those described by Watanabe *et al.* (11). A chimeric plasmid (pJDB-ADH-L10-HSA-A) having a cDNA for the mature form of HSA along with an L10 leader sequence was a gift from Tonen Co. (Tokyo, Japan). The mutagenic primer used (underlined letters indicate mismatches) was 5′-CTTCAGCAGTCTCCATTTGAAG-3′. The L10-HSA coding region was amplified by PCR with a forward and a reverse primer carrying a 5′-terminal EcoRI site and cloned into the EcoRI-digested pKF19k vector (Takara Shuzo Co., Kyoto, Japan). Mutagenesis was performed with a site-directed mutagenesis kit (oligonucleotide-directed dual amber method) obtained from Takara Shuzo Co. The mutation was confirmed by DNA sequencing of the entire HSA coding region with the dideoxy chain termination method on a PerkinElmer ABI Prism 310 Genetic Analyzer. For constructing the HSA expression vector pHIL-D2-HSA, an L10-HSA coding region without or with the desired mutation site was incorporated into the methanol-inducible pHIL-D2 vector (Invitrogen Co., San Diego, CA, USA). The resulting vector was introduced into the yeast species *P. pastoris* (strain GS115) to express rHSA. Secreted rHSA was isolated from the growth medium by a combination of precipitation with 60% (w/v) $(NH_4)_2SO_4$, followed by purification on a Blue Sepharose CL-6B column (Amersham Pharmacia Co., Uppsala, Sweden). Isolated protein was defatted using the charcoal procedure described by Chen (9), deionized, freeze-dried and then stored at −20°C until used. The resulting albumins (treated with dithiothreitol) appeared as a single band on SDS/PAGE and all the recombinant proteins migrated at the same position as native HSA. Density analysis of protein bands stained with Coomassie Brilliant Blue showed that the purity of the recombinant albumins was in excess of 97%.

HPLC System

An ion exchange HPLC system was used in this study. The system was used to examine the redox state of albumin in serum and consisted of a Model MIX 100 double-plunger pump and a Model FP-2025 fluorescence detector (excitation wavelength, 280 nm; emission wavelength, 340 nm), in conjunction with a Model PU-2080 system controller, all obtained from Jasco Co., Tokyo, Japan. A Shodex Asahipak ES-502N (Showa Denko Co., Tokyo, Japan) ion-exchange column was used. The column temperature was 37°C. Measurements were carried out by solvent gradient elution with increasing ethanol concentrations from 0 to 5% in 0.05 M sodium acetate-0.40 M sodium sulfate (pH 4.85) and a flow rate of 1.0 mL/min. Samples were injected with fixed volumes of 5 μl of serum. To determine the value for each fraction of albumin, (i.e., f(HMA) = [HMA:(HMA + HNA-1 + HNA-2)], f(HNA-1) = [HNA-1:(HMA + HNA-1 + HNA-2)], and f(HNA-2) = [HNA-2:(HMA + HNA-1 + HNA-2)]) the HPLC profiles obtained were subjected to numerical curve fitting; each peakshape was approximated by a Gaussian function. The Student's *t*-test was used to evaluate the significance of the differences. Values are expressed as mean ± SD (12).

Oxidation of HSA and Serum by Chloramine-T

To prepare CT-HSA, HSA (15 μM) was incubated for 1 h in phosphate buffer (pH 8.0) at 37°C in an oxygen-saturated solution containing 0.1 mM ($CT_{0.1}$-HSA), 1 mM (CT_1-HSA), 10 mM (CT_{10}-HSA) or 50 mM (CT_{50}-HSA) chloramine-T. After incubation, the oxidation reactions were stopped by cooling followed by extensive dialysis of solutions against water. The control involved incubating albumin dissolved in buffer alone, and in all cases the proteins were freeze-dried after dialysis and stored at −20°C until used.

Amino Acid Residues Oxidized

Reactivity of ^{34}Cys Residue with DTNB

Albumin solutions 1.0×10^{-4} M, 2 mL 0.067 M phosphate buffer) were preincubated at 37°C. Absorbance increases at 412 nm were monitored against time after the addition of DTNB (final concentration 2.0×10^{-4} M) (13).

Oxidation of Met Residues

Oxidized HSA, mutated rHSA, and control albumins, all at a concentration of 10 μM, were reduced with dithiothreitol (100 mM) in the presence of EDTA (10 mM) in denaturing

buffer (6 M guanidine hydrochloride in 0.25 M Tris, pH 8.0). The samples were incubated for 16 h at 37°C. After this treatment, the albumins were pyridylethylated and then digested with CNBr (CNBr: Met molar ratio of 200:1) in the dark for 24 h at 37°C. The digestions were stopped by the addition of acetone. After evaporation of the acetone and washing with ethanol, the proteins were dissolved in 0.1% trifluoroacetic acid. Protein concentrations were determined by a Bradford assay (14), and the same amounts of proteins were used in the SDS-PAGE analysis. It is evident that the cleavage of oxidized HSAs was suppressed by the oxidation of Met residues.

Changes in Protein Net Charge

Changes in the net charge of albumin were evaluated by a modification of the capillary electrophoresis method described by Pande *et al.* (15). One mL of an albumin sample (2 μM) was run in 100 mM borate buffer (pH 9.0 and 20°C), and the migration time was determined by means of a CE990/990-10 type capillary electrophoresis from Jasco Co. (Tokyo, Japan).

Carbonyl Group Determination

Protein-bound carbonyl groups were quantitated using the method of Climent *et al.* (1). In summary, the groups were derivatized with fluoresceinamine and their number calculated from the absorbance of the complexes at 490 nm (Jasco Ubest-35 UV/VIS spectrophotometer).

Structural Properties of Native, Oxidized, and Mutant HSAs

Circular Dichroism (CD)

Measurements were done using a Jasco J-720 type spectropolarimeter (Jasco Co., Tokyo, Japan) at 25°C. Far-UV and near-UV spectra were recorded at protein concentrations of 20 μM in phosphate buffer using 1 mm and 1 cm quartz cells, respectively.

Effective Hydrophobicity of Native, Oxidized, and Mutant HSAs

The effective hydrophobicity of the albumins (1 μM), as dissolved in phosphate buffer, was probed with bis-ANS (10 μM) at 25°C. The compound was excited at 394 nm (16), and fluorescence spectra were recorded on a Jasco FP-770 fluorometer (Tokyo, Japan) using 1 cm quartz cells, thermostated devices and 5 nm excitation and emission band widths.

Effect on Aromatic Amino Acid Residues

Steady-state fluorescence measurements were made using a Jasco FP-770 fluorometer with 1 cm quartz cells and thermostated devices. All studies were performed using a protein concentration of 2 μM at 25°C using 5 nm excitation and emission band widths. A fluorescence excitation wavelength of 295 nm (tryptophan (Trp) residue) or 280 nm (tyrosine (Tyr) residues) was employed.

Absorbance spectra (200–400 nm) of the albumins (20 μM) were recorded at 25°C with 1 cm quartz cells by using the Jasco UV/VIS spectrophotometer.

Functional Properties of Native, Oxidized, and Mutant HSAs

Ligand Binding Experiments

To study the binding of ligands to the albumins, warfarin or ketoprofen was added to a solution of albumin (10 μM) in phosphate buffer to give a final drug concentration of 5 μM. The unbound ligand fractions were separated using an Amicon MPS-1 micropartition system with YMT ultrafiltration membranes by centrifugation (2000 g, 25°C, 40 min). Adsorption of warfarin or ketoprofen to the filtration membranes and apparatus was found to be negligible. The concentration of unbound ligand was determined by HPLC. The HPLC system consisted of a Hitachi 655A-11 pump and a Hitachi F1000 variable fluorescence monitor or a Hitachi 655A variable wavelength UV monitor. LiChrosorb RP-18 (Cica Merck, Tokyo, Japan) was used as the stationary phase. The mobile phase consisted of 200 mM sodium acetate buffer (pH 4.5)/acetonitrile (40:60, v/v) for warfarin and of 200 mM sodium acetate buffer (pH 4.5)/acetonitrile (60:40, v/v) for ketoprofen. The flow rates in both cases were 1 mL/min. Warfarin was quantitated fluorometrically by using 320 nm and 400 nm for excitation and emission, respectively, and ketoprofen was detected at 270 nm by means of UV monitoring. The unbound fraction (%) was calculated as follows: Unbound fraction (%) = [ligand concentration in filtered fraction/total ligand concentration (before ultrafiltration)] × 100.

Determination of Esterase-Like Activity

The reaction of *p*-nitrophenyl acetate with the albumins was followed spectrophotometrically at 400 nm (Jasco Ubest-35 UV/VIS spectrophotometer) by monitoring the rate of appearance of *p*-nitrophenol. The reaction mixtures contained 5 μM *p*-nitrophenyl acetate and 20 μM protein in phosphate buffer. Reactions were followed at 25°C. Under these conditions, a pseudo-first-order rate constant analysis could be applied (17), and the apparent hydrolysis rate constants (k_{obs}) were calculated.

***In Vivo* Experiments**

Animals

Male ddY mice (6-weeks old, 25–35 g) were purchased from the Shizuoka Agricultural Cooperative Association for Laboratory Animals (Shizuoka, Japan). The animals were maintained under conventional housing conditions. This study was carried out in accordance with the Principles of Laboratory Animal Care as adopted and promulgated by the United States National Institutes of Health.

Biodistribution Experiment

HSAs were radiolabeled with ^{111}In using DTPA anhydride as described previously (18). Each radiolabeled derivative was purified by gel-filtration chromatography using a Sephadex G-25 column eluted with 0.1 M acetate buffer (pH 6.0). The absorbency of the eluants was measured at 280 nm, and the protein-containing fractions were pooled. The resulting solution was concentrated and washed with 0.9% NaCl by ultrafiltration. The specific activity of each derivative was ap-

proximately 37 MBq/mg protein. The mice received a 0.1 mg/kg dose of a ^{111}In-HSA conjugate in saline by tail vein injection and were housed in metabolic cages for urine collection. At given time points, blood was collected from the vena cava with the animal under ether anesthesia, and plasma was obtained by centrifugation. The heart, lung, liver, spleen, and kidney were excised, rinsed with saline, weighed, and examined for radioactivity. The amount of radioactivity in urine was determined by collecting urine both excreted and remaining in the bladder. ^{111}In radioactivity was counted in a well-type NaI scintillation counter (ARC-500; Aloka, Tokyo, Japan).

Pharmacokinetic Analysis

Tissue distribution patterns of the ^{111}In-HSA derivatives were evaluated using organ uptake clearance according to a previous reported method (19). In the early period after injection, the efflux of ^{111}In radioactivity from organs is assumed to be negligible, because the degradation products of ^{111}In-labeled ligands using DTPA anhydride cannot easily pass through biological membranes (19). This assumption was supported by the fact that no ^{111}In was detectable in the urine. Using this assumption, organ uptake clearance was calculated by dividing the amount of radioactivity in an organ at 120 min by the area under the plasma concentration-time curve (AUC) at the same time point. AUC was calculated by fitting an equation to the plasma concentrations of the derivatives using the nonlinear least-squares program MULTI (20). Tissue distribution patterns were evaluated using tissue uptake clearances according to the integration plot analysis. Tissue accumulation at time t was proportional to the $AUC_{0\text{-}t}$. By dividing the tissue accumulation at time t (χt) and the $AUC_{0\text{-}t}$ by the plasma concentration (Ct), CL tissue was obtained from the slope of the plot of $\chi t/Ct$ versus $AUC_{0\text{-}t}/Ct$. A previous report (21) has shown, that ^{111}In is not suitable for evaluating the dynamic phase of a protein for which the *in vivo* half life is long. Therefore, we estimated the plasma half-life and liver clearance within the 120 min, period.

Statistics

Where possible, statistical analyses were performed using the Student's *t* test.

RESULTS

HPLC Studies on Serum and Oxidized Serum From Healthy Young Subjects

Figure 1 shows a representative HPLC profile of serum and oxidized serum from a healthy young subject, obtained by elution from an ES-502N column with an increasing ethanol concentration from 0 to 5% in the acetate-sulfate buffer (pH 4.85). Peaks 1, 2, and 3 in Fig. 1 correspond well to HMA, HNA-1, and HNA-2 with the retention times of 15.8, 25.8, and 31.2 min, respectively (Fig. 1). Increasing the chloramine-T concentration from 0 mM to 0.1 or 1 mM resulted in an increase in, especially, HNA-2 (Table I). When the chloramine-T concentration was increase to 10 or 50 mM (Table I), or the exposure time was increased from 3 min to 1 h (Fig. 1), the three protein peaks disappeared. The reason is that, under these conditions, HSA was modified to such an extent

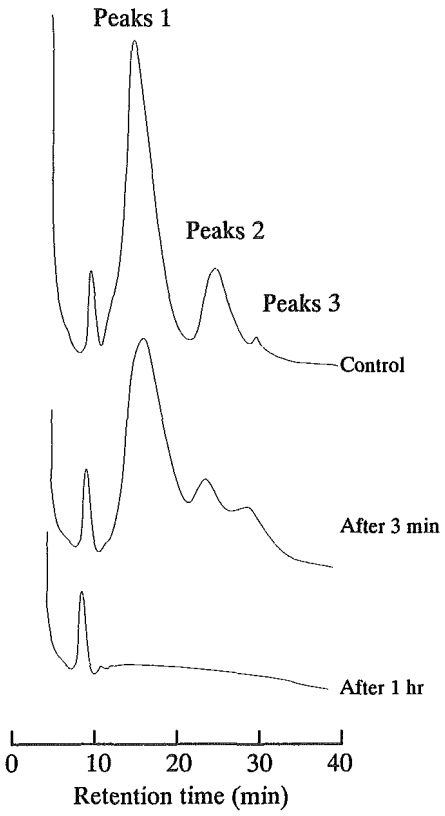

Fig. 1. HPLC profile of control serum and sera exposed to chloramine-T (1 mM) for 3 min or 1 h. The serum was from a healthy young male subject (23 years of age) and was eluted from an ES-502N column with an ethanol gradiant of 0 to 5% in acetate-sulfate buffer (pH 4.85). The ethanol concentration gradient was as follows; 0–5 min, 0%; 5–30 min, linear increase from 0 to 5%; 30–35 min, linear decrease from 5 to 0%; 35–40 min, 0%. Peaks 1, 2, and 3 correspond to HMA, HNA-1 and HNA-2, respectively, and their relative values are included in Table I.

that it remained bound to column and could only be eluted at a high ethanol concentrations (not shown).

Extent of Oxidation of Amino Acid Residues

The effect of oxidation on the reactivity of ^{34}Cys was examined using DTNB. The reactivity constants for pure HSA and rHSA were found to be the same (i.e., 0.07 min^{-1}). The constant was decreased only slightly for $CT_{0.1}$-HSA (i.e., 0.05 min^{-1} $P < 0.05$), and considerably decreased in the case of CT_1-HSA and CT_{10}-HSA (i.e., 0.02 min^{-1}; $P < 0.001$), and no reactivity at all could be detected for CT_{50}-HSA. As expected, no reactivity was found for the C34S mutant. These results indicate an increased oxidation of the cysteine residue with increasing concentrations of chloramine-T.

To examine the potential effect of the oxidations on the six Met residues of albumin, the proteins were reduced and treated with CNBr and then examined by SDS-PAGE. As seen in Fig. 2, the C34S mutant (lane 2) and $CT_{0.1}$-HSA (lane 3) showed the same fragmentation pattern as normal HSA (lane 1) and wild-type rHSA (not shown). However, in the case of CT_1-HSA (lane 4), a slight decrease in the amount of low-molecular weight fragments and a corresponding increase in high-molecular weight fragments and intact protein were observed. This tendency is more pronounced at higher con-

Table I. f(HMA), f(HNA-1) and f(HNA-2) Values (%) for HSA and Oxidized HSA in Serum from Normal Subjects[a]

	Serum	Serum + CT (0.1 mM)	Serum + CT (1 mM)	Serum + CT (10 mM)	Serum + CT (50 mM)
After 3 min					
f(HMA)	74.9 ± 0.99	72.4 ± 2.50	65.2 ± 3.38*	N.D.[b]	N.D.
f(HNA-1)	22.1 ± 1.51	22.5 ± 1.38	22.4 ± 3.95	N.D.	N.D.
f(HNA-2)	2.97 ± 1.03	2.62 ± 0.78	12.4 ± 1.28*	N.D.	N.D.
After 1 h					
f(HMA)	72.8 ± 2.11	61.2 ± 3.63*	N.D.	N.D.	N.D.
f(HNA-1)	23.9 ± 2.39	23.7 ± 4.23	N.D.	N.D.	N.D.
f(HNA-2)	3.21 ± 1.13	14.6 ± 1.23*	N.D.	N.D.	N.D.

[a] Average values of five experiments (± S.D.).
[b] N.D. denotes for not detectable.
* $P < 0.001$ as compared with Serum.

centrations of chloramine-T (lanes 5 and 6). These results show a concentration-dependent oxidation of methionine residues.

The net charge on the albumins was investigated by determining their migration times by capillary electrophoresis. The migration times for the C34S mutant (18.59 ± 0.11 min), $CT_{0.1}$-HSA (18.66 ± 0.08 min), CT_1-HSA (18.46 ± 0.04 min) and CT_{10}-HSA (18.45 ± 0.04 min) were the same or similar to that of HSA and rHSA (18.59 ± 0.11 min and 18.58 ± 0.19 min). By contrast, the migration time for CT_{50}-HSA was increased significantly (20.03 ± 0.42 min, $P < 0.005$). Thus, the net negative charge on albumin is increased, only at the highest chloramine-T concentrations used.

The oxidation of proteins frequently results in the formation of carbonylated amino acid residues. Therefore, the formation of such groups was measured as a function of chloramine-T concentration. The results (mol carbonyl groups/mol protein) showed concentration-dependent increases in the level of these groups: 0.098 ± 0.045 for $CT_{0.1}$-HSA, 0.158 ± 0.030 for CT_1-HSA, 0.331 ± 0.013 for CT_{10}-HSA and 0.769 ± 0.038 for CT_{50}-HSA. In comparison, the level in control HSA was only 0.045 ± 0.017.

Structural Properties of Native, Mutant, and Oxidized HSAs

The structural properties of the albumins were examined using several different spectroscopic methods. Figures 3A and 3B show the far-UV and near-UV CD spectra, respectively. As can be seen in Fig. 3A, the characteristics of the CD spectra of the C34S mutant, rHSA, $CT_{0.1}$-HSA and CT_1-HSA were similar to that of native HSA. In the case of CT_{10}-HSA and CT_{50}-HSA, the θ_{obs}-values are slightly higher in the range ca. 207–240 nm indicating some loss in α-helix structure. However, in all cases, the spectra were very different from that obtained for albumin, when dissolved in phosphate buffer, pH 7.4, containing 6 M guanidine hydrochloride. Fig. 3B shows that the tertiary structures of CT_{10}-HSA and CT_{50}-HSA, but not that of the other samples, had been modified. However, again the structural changes are not so pronounced as those observed for albumin that had been denatured with guanidine hydrochloride.

The effect of oxidation on the exposure of hydrophobic areas was examined using the fluorescence probe bis-ANS. The results (Fig. 4A) indicate that neither the mutation of ^{34}Cys nor oxidation at the low chloramine-T concentrations had any measurable effect on the accessible albumin hydrophobicity. However, treatment with higher concentrations of chloramine-T (CT_{10}-HSA and CT_{50}-HSA) resulted in an increase in accessible hydrophobic regions.

The effect of mutating ^{34}Cys and of the oxidations on the intrinsic fluorescence of albumin is shown in Fig. 4B. This fluorescence, which mainly is due to the excitation of ^{214}Trp, is only affected to a small extent by the mutation and treatment with 0.1 mM or 1 mM chloramine-T. In contrast, 10 mM

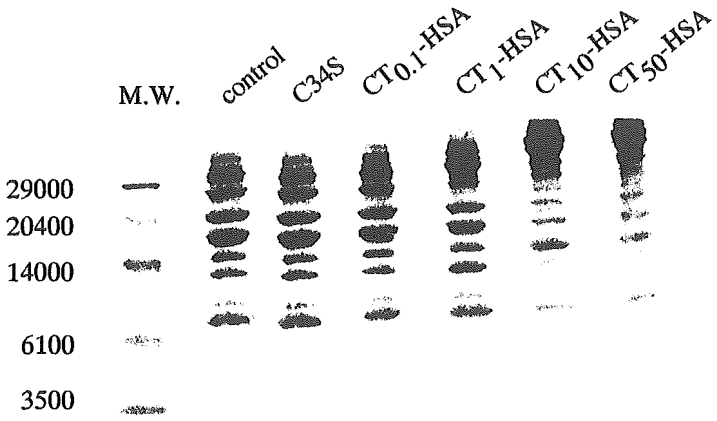

Fig. 2. SDS-PAGE electrophoresis of the reduced forms of control albumin (HSA = rHSA), the C34S mutant and chloramine-T oxidized HSAs treated with CNBr. Left lane, molecular weights of protein markers (M.W.). The gel was stained Coomassie Brillant Blue.

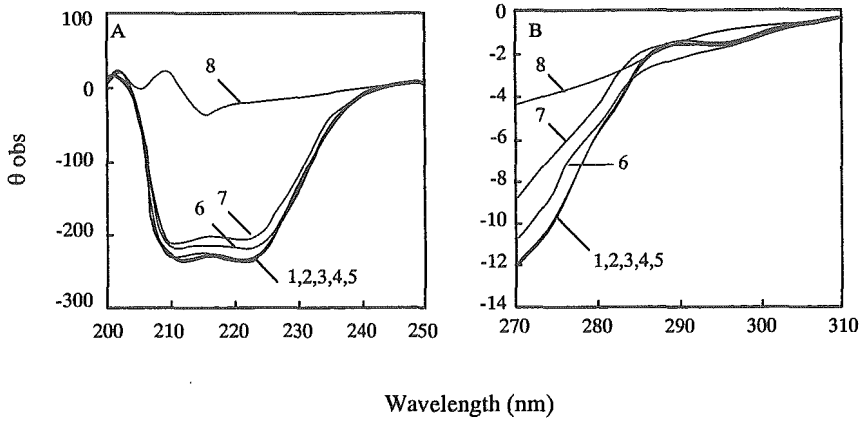

Fig. 3. Far-UV (A) and near-UV CD spectra (B) of native, mutated or oxidized HSAs. (1) native HSA, (2) wild-type rHSA, (3) the C34S mutant, (4) $CT_{0.1}$-HSA, (5) CT_1-HSA, (6) CT_{10}-HSA, (7) CT_{50}-HSA, (8) native HSA dissolved in phosphate buffer, pH 7.4, containing 6 M guanidine hydrochloride. Spectra are the averages of three determinations.

and especially 50 mM chloramine-T had a pronounced effect on the fluorescence spectrum. The fluorescence at λ_{max} was decreased to 76.8% and 23.8% of the normal level, respectively, and the λ_{max} was blue shifted in both cases from 339 nm to 333 nm. These findings suggest that in CT_{10}-HSA and CT_{50}-HSA minor conformational changes occurred in the vicinity of the Trp residue. However, the possibility that the Trp residue itself could have been oxidized cannot be excluded. The type of changes in light absorption spectra (data not shown) suggest that this seems to be the case for CT_{10}-HSA and CT_{50}-HSA (4).

The nature of the Tyr residues in the different albumins was examined by fluorescence measurements using an excitation wavelength of 280 nm and emission wavelengths from 290 nm to 370 nm (data not shown). In this case no effects as the result of the mutation or oxidations seem to have taken place.

Functional Properties of Native, Mutant and Oxidized HSAs

The unique drug binding properties of HSA can, to a great extent, be explained by the presence of two major binding sites; Site I and Site II (22), which are located within specialized cavities in subdomain IIA and IIIA, respectively (3). The potential effects of mutation and oxidation at these sites were examined using warfarin and ketoprofen as representative drugs. As seen in Table II, the high-affinity binding of warfarin which takes place at site I (23), was not affected by the mutation or mild oxidation by chloramine-T. However, binding was slightly decreased by a more severe oxidation of HSA (CT_{10}-HSA and CT_{50}-HSA). Essentially, the same effects, but to a more dramatic extent, were observed for the high-affinity binding of ketoprofen (Table II) which takes place at Site II (24).

Among its many functional properties HSA also possesses an esterase-like activity that is largely due to the close proximity of ^{410}Arg and ^{411}Tyr in Site II (17). Figure 5 shows that this activity is significantly reduced in the case of CT_{10}-HSA and, especially, CT_{50}-HSA, whereas the remaining albumins have comparable activities.

Pharmacokinetic Analysis of Native, Mutant, and Oxidized HSAs

In an attempt to evaluate whether the C34S mutation or the chloramine-T induced oxidations had any effect on the biological fate of HSA, plasma half-lifes and uptake clearance

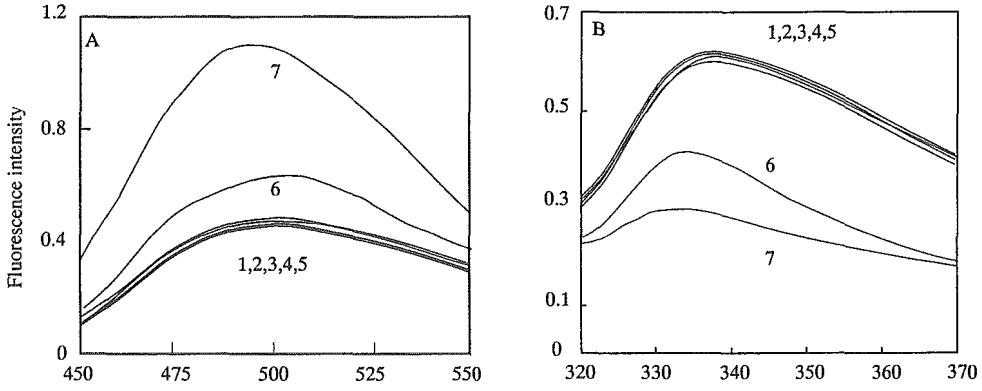

Fig. 4. Effect of different protein modifications on the fluorescence of albumin-bound bis-ANS (A) and on the intrinsic fluorescence of albumin as excited at 295 nm (B). (1) native HSA, (2) wild-type rHSA, (3) the C34S mutant, (4) $CT_{0.1}$-HSA, (5) CT_1-HSA, (6) CT_{10}-HSA, (7) CT_{50}-HSA. Spectra are the averages of three determinations.

Table II. Binding of Warfarin and Ketoprofen to Native, Mutated and Oxidized HSAs at pH 7.4 and 25°C[a]

Protein	Free fraction (%) (warfarin)	Free fraction (%) (ketoprofen)
Native HSA	24.71 ± 2.07	3.78 ± 0.52
Wild-type rHSA	25.48 ± 1.14	3.92 ± 0.67
C34S	25.01 ± 1.33	3.99 ± 1.17
$CT_{0.1}$-HSA	26.54 ± 1.93	3.83 ± 2.11
CT_1-HSA	27.41 ± 0.93	3.89 ± 2.34
CT_{10}-HSA	31.26 ± 1.54***	33.9 ± 2.44**
CT_{50}-HSA	35.60 ± 1.01**	46.5 ± 3.58*

[a] Average values of three experiments (± S.D.). * P < 0.001, ** P < 0.01 and *** P < 0.05 all as compared with native HSA.

Table III. Half-Lifes and Liver Clearances of ^{111}In-HSAs in Mice[a]

Protein	Half-life (min)	Liver uptake clearance (μL/h)
Native HSA	20.7 ± 1.26	13.37 ± 2.57
Wild-type rHSA	20.1 ± 2.85	13.47 ± 2.71
C34S	19.2 ± 1.39	14.00 ± 1.37
$CT_{0.1}$-HSA	20.8 ± 1.40	12.15 ± 1.98
CT_1-HSA	20.5 ± 2.40	13.17 ± 1.86
CT_{10}-HSA	20.3 ± 2.93	12.93 ± 2.12
CT_{50}-HSA	8.69 ± 1.39*	146.0 ± 8.91*

[a] Average values of three experiments (± S.D.). * P < 0.001 as compared with native HSA.

of the HSAs were determined in mice (Table III). Except for CT_{50}-HSA, the albumins had the same half-life (i.e., about 20 min). To better understand the reason for the decreased plasma half-life of CT_{50}-HSA (8.69 min) organ uptakes was studied. In Table III, the decreased plasma half-life of CT_{50}-HSA can be explained by a very pronounced increment in liver clearance. By contrast, neither the mutation nor the milder oxidation of albumin had any effect on liver clearance. The uptake by heart, lung, spleen, and kidney of CT_{50}-HSA, and the other modified albumins, were comparable to those of native albumin (results not shown).

DISCUSSION

The Validity of Chloramine-T as an Oxidant

Albumin, which is thought to have antioxidant properties, is the most abundant protein in extracellular fluids. Oxidation of protein sulfhydryl groups to mixed disulfides and their conversion to sulfhydryls by reduction might represent an effective antioxidant system in extracellular fluids. In this sense, albumin, which possess a single sulfhydryl residue (^{34}Cys), is responsible for the largest fraction of reactive sulfhydryl groups in extracellular fluids and the mercaptnonmercapt conversion (intermolecular sulfhydryl disulfide exchange reaction) of serum albumin might be a component in such a system. In this study, the authors attempted to construction *in vivo* oxidation model of albumin by treatment with CT using on HPLC system. As shown in Fig. 1, in the case of serum treated with CT (1 mM) for 3 minutes, the f(HMA) value of 65.2% was significantly lower than that of 74.9% for healthy young male subjects. A significant decrease in the f(HMA) value as a result of aging and some diseases has previously been reported (10,12). The HPLC profile observed in Fig. 1 was similar to that of serum treated with CT (0.1 mM) for 1 h (Table. I). This finding leads to the suggestion that the oxidation of HSA is dependent on the concentration of oxidant as well as incubation time used for the oxidation and that HSA treated with CT for extended periods is easily oxidized even when low concentration of oxidant are used. Therefore, the authors used this oxidant and carried out a detail examination of the importance of ^{34}Cys and other residues relative to antioxidant properties of HSA.

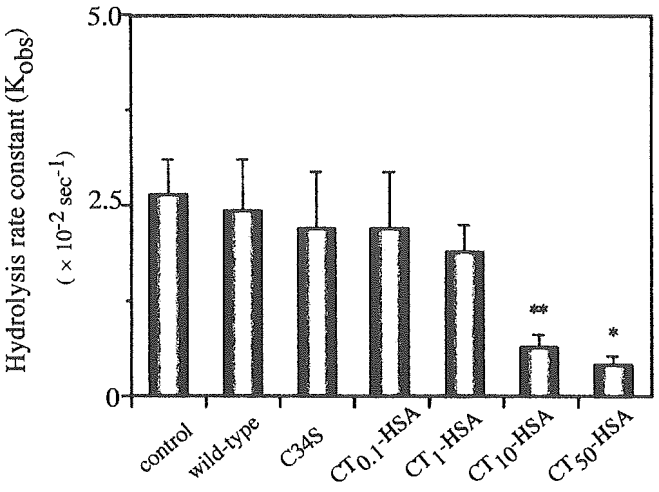

Fig. 5. Effect of mutation and oxidation on the rate constants (K_{obs}) for the hydrolysis of *p*-nitrophenyl acetate by albumin at pH 7.4 and 25°C. The data are average values of three experiments (± S.D.). * P < 0.001 and ** P < 0.01 both as compared with control.

Amino Acid Residues Oxidized

The type and number of oxidized amino acid residues of HSA increase with the chloramine-T concentration. The active oxidants in this system are HO· and chloro radicals (4). In $CT_{0.1}$-HSA and CT_1-HSA, only ^{34}Cys and Met residues were affected. Increasing the chloramine-T concentration to 10 mM oxidized Met residues were affected to a more pronounced extent and apparently affected ^{214}Trp as well. Finally, in CT_{50}-HSA no reactivity of ^{34}Cys was detected, Met residues and ^{214}Trp (or its surroundings) were intensively modified and the net charge of HSA became more negative. The latter observation is explained by the oxidation of arginine, lysine, or proline residues to λ-glutamyl semialdehyde (1).

Structural Properties

The mild oxidation of HSA ($CT_{0.1}$-HSA and CT_1-HSA) has no measurable effect on its secondary and tertiary structures. However, in CT_{10}-HSA and, especially, CT_{50}-HSA slight decreases in α-helical contents were observed accompanied by tertiary conformational changes. These were detectable by near-UV CD and resulted in an increased exposure of hydrophobic portions of the protein. Large changes in intrinsic fluorescence and light absorption spectra were also observed. Although these changes are consistent with oxidation of ^{214}Trp, they could also, at least partly, reflect conformational changes in the protein in the vicinity of that residue.